A SUCCESSFUL REPLACEMENT OF CONVENTIONAL ORGANOPHILIC CLAY WITH A NEW POLYMER AS VISCOSIFIER AND FILTRATION CONTROL AGENT IN MINERAL-OIL-BASED DRILLING MUDS

A Thesis

by

JAIRO A. CORTES

Submitted to the Office of Graduate and Professional Studies of
Texas A&M University
in partial fulfillment of the requirements for the degree of

MASTER OF SCIENCE

Chair of Committee,	Hisham Nasr-El-Din
Committee Members,	Jerome Schubert
	Mahmoud El-Halwagi
Head of Department,	Jeff Spath

August 2018

Major Subject: Petroleum Engineering

ABSTRACT

Oil-based drilling fluids (OBDF) can enhance wellbore stability in water-sensitive reservoirs and protect metal surfaces of drilling equipment to minimize corrosion due to H_2S and CO_2. Components of OBDF include oil as the continuous phase and water as the dispersed phase, in conjunction with viscosifiers, emulsifiers, filtration control agents, and weighting materials. Two of the most common types of continuous phases in oil-based drilling fluids are diesel and mineral oil. Mineral oil is less toxic than diesel, and oil retention properties of OBDF with mineral oil are less than OBDF with diesel. Organophilic clays are clay minerals that have been treated with oil-wetting agents, which will make the clay oil-dispersible. Organophilic clays mixed in OBDF do not exhibit same viscosity or suspension characteristics as in water-based drilling fluids, because electrical interaction between particles is minimal, making it difficult to build viscosity and gel strength in high pressure and high temperature (HP/HT) wellbore conditions. A new mineral-oil-based drilling fluids (MOBDF) proposed was obtained by the successful replacement of conventional organophilic clay additives with a methylstyrene/acrylate copolymer.

Two different drilling fluid formula, one containing conventional organophilic clay additives and the other containing the replacement polymer as a viscosifier and filtration control agent, were hot rolled at 150°F for 16 hours. To evaluate the alteration of the wettability caused by the MBDOF and its components contact-angle measurements were made in the laboratory. With similar weight proportions, the apparent and kinetic viscosities of organophilic clay and cross-linked polymer were also

compared.

Rheological properties and filtration characteristics tests were conducted using a rotational viscometer and a HP/HT filter press, under three simulated wellbore conditions (140°F/ 300 psi, 190°F/300 psi, and 250°F/500 psi). Filter cake is formed due to positive pressure between OBDF and pore throat pressure. As a barrier between wellbore and formation, it can minimize solids and fluids invasion. A core flooding test was conducted to evaluate permeability of the filter cakes and CT scan was used to measure the density distribution of the filter cakes. Emulsion droplets formed by mixing MOBDF filtrate fluids with formation water were observed to analyze emulsion plugging damage.

Experimental results show that the novel polymer has a promising future of practical application, by providing thermal stability and stable rheological properties for MOBDF in HP/HT conditions. It also yields lower filtration volume, higher quality filter cake and a slightly greater emulsion plugging capabilities and greater formation permeability retention than organophilic clay-based drilling fluids.

DEDICATION

I would like to dedicate this project to:

My beloved mother Daissy, my source of inspiration.

My brother Johnny, my best friend.

My fiancé Sofía, my love, happiness, and unconditional support.

Thank you all for your everlasting love and warm encouragement throughout this process.

God bless you.

ACKNOWLEDGEMENTS

I would like to express my sincere thanks and appreciation to Dr. Hisham Nasr-El-Din for his invaluable guidance and support during my stay at Texas A&M University and for serving as chair of my advisory committee.

I would like to extend my gratitude to Dr. Jerome Schubert and Dr. Mahmoud El-Halwagi for serving as members of the advisory committee and for their vital cooperation throughout the course of this research.

Finally, I would like to thank my good friends and colleagues Jing Zhou, Tariq Almubarak, Omar Mahmoud, Ahmed Elsarawy, Mina Shaker, and my TAMU Colombian family for making this such a wonderful experience.

CONTRIBUTORS AND FUNDING SOURCES

Contributors

This work was supported by a thesis committee consisting of Professors Dr. Hisham Nasr-El-Din and Professor Jerome Schubert of the Department of Petroleum Engineering and Professor Mahmoud El-Halwagi of the Department of Chemical Engineering.

All work for the thesis was completed by the student, in collaboration with Professor Hisham Nasr-El-Din of the Department of Petroleum Engineering and the assistance of PhD candidate Jing Zhou.

Funding Sources

Graduate study was supported by a fellowship from Texas A&M University

NOMENCLATURE

API	American Petroleum Institute
BHA	Bottom hole assembly
CT scanner	Computed tomography scanner
CTN	CT number
ECD	Equivalent circulating density
HP/HT	High pressure/high temperature
MODF	Mineral oil-based drilling fluid
OBDF	Oil-based drilling fluid
OBM	Oil-based mud
P	Pressure
psi	lb/in^2
PV	Plastic viscosity, Pore Volume
RPM	Revolutions per minute
ROP	Rate of penetration
S.G.	Specific gravity
SBF	Synthetic-based fluids
T	Temperature
vol.%	Volume percent
wt%	Weight percent
WBDF	Water-based drilling fluid
WBM	Water-based mud
XRD	X-ray diffraction
YP	Yield point

TABLE OF CONTENTS

Page

LIST OF FIGURES

Page

LIST OF TABLES

Page

1. INTRODUCTION

The success of the completion of an oil or gas well and its cost depends substantially on four principal factors:

1. Bit rate of penetration (ROP)
2. Drill bit cleaning, cooling and lubrication
3. Drill cutting suspension and transportation to the surface
4. Support or integrity of the wellbore

Drilling fluids, also referred to as drilling muds, are added to the wellbore to facilitate the drilling process affecting all the factors previously mentioned. The drilling fluid's density and ability to penetrate the formation have an effect on the rate of the penetration. The hydraulic energy expended on the bottom of the hole and the apparent viscosity and flow rate of the drilling fluid affect the cutting transport. The ability of the fluid to form an impermeable filter cake and the ability to control formation pressures affect and the stability and integrity of the wellbore (De Stefano 2013).

The continuously increasing worldwide demand for energy over the past decade has driven oil and gas companies to drill deeper and hotter wells. As wells get deeper, drilling fluids have taken on increased importance, serving a number of purposes and solving a variety of problems that vary greatly from place to place. Operating under these harsh conditions has motivated our industry to develop new robust drilling fluid systems capable of safely performing under these circumstances.

Oil-based drilling fluids were developed to help maximize rates of penetration, increase lubricity in directional and horizontal wells, and minimize wellbore stability problems such as those caused by reactive shales. Until operators began drilling in deep water locations, where the pore pressure/fracture gradient (PP/FG) margin is often very narrow, the standard formulations provided satisfactory performance (Golis 1984). Consistent rheology is crucial for the successful construction of these oil/gas wells. High pump pressures mean high equivalent circulating densities (ECDs) at the bottom of the well, increasing the probability of losses. Fluid losses in deep water wells can be costly, considering the difficult logistics (Dhanashree Kulkarni and Shadaab Maghrabi 2014).

1.1 Problem Statement

When drilling deep wells, a narrow drilling margin (mud-weight windows) is a key challenge to the drilling operation, thus the selection of the drilling fluid system is crucial. The selected fluid system must be capable of delivering low equivalent circulating density (ECD) margins to mitigate the risk of exceeding the formation fracture gradient (Mahrous et al. 2016), a more stable and controllable fluid rheology (Burrows et al. 2004), and economically viable.

Oil-based drilling fluids containing organophilic clays additives do not exhibit same viscosity or suspension characteristics as in water-based drilling fluids due to the electrical interaction between particles is minimal, making it difficult to build viscosity and gel strength in high pressure and high temperature (HP/HT) wellbore conditions (Schmidt et al. 1987).

By switching from a standard oil-based drilling fluid, containing organophilic clay additives, to the use of a novel clay-free mineral oil-based drilling fluid (MBODF), the drilling operation will benefit from a drilling fluid capable of performing under these desired conditions, an overall reduction in logistics; a reduction in volume of fluid and material needed, along with higher rates of penetration (ROP) due to lower equivalent circulating densities (ECDs), and form a non-damaging thin filter cake that would eliminate the need for costly and time consuming clean-up treatments (Martini et al. 2017).

Organophilic clays are most widely used as primary viscosifier for oil-based drilling fluids and synthetic-based drilling fluids. Bentonite is an organophilic clay that has been treated with an amine to make it yield in oil. However, organophilic clay requires significant shear and circulating time to yield fully. Overtreatment resulting from this delayed response often causes excessive viscosity, and the problem is compounded when the fluid is at ambient temperature or worse, is exposed to cold temperatures at the seabed in deep water locations (Methven and Baumann 1972).

There is a need to develop a fluid that produces higher gel strengths initially and maintains a relatively flat response to temperature throughout the complete temperature cycle of the drilling operation. Organophilic clays do not provide the viscosity or suspension characteristics in the same way that clay solids do in water-based fluids.

1.2 Antecedents

In 2001, Burrows et al. (2004) first introduced an oil-based mud formulated entirely without commercial clays or lignites in the Gulf of Mexico. Rheological properties were controlled through the emulsion characteristics; a radical departure from accepted solids suspension mechanisms. The behavior of this unique fluid changed the perception about what constitutes a "good mud."

The clay-free, emulsion-based fluid system consistently prevented detectable barite sag on 80+ wells drilled. Based on observed fluid densities after long static periods (an 8-day logging run in one case) and verified by modular dynamic test (MDT) log data on numerous high-angle wells, the fluid's unique emulsion structure and wetting characteristics prevented settling of barite and other solids as shown in Figure 1.

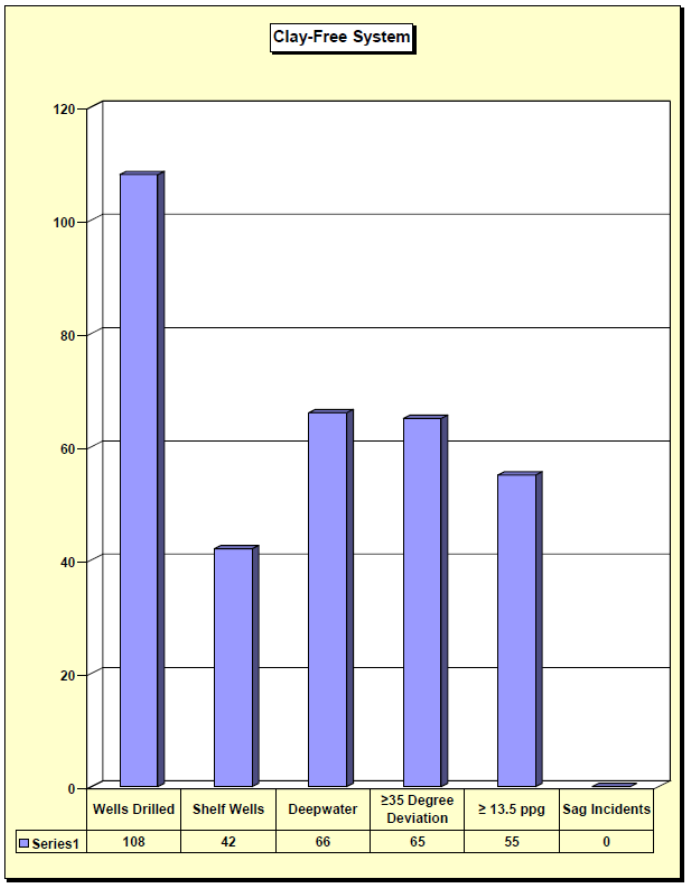

Figure 1. Zero barite sag incidents on wells drilled with clay-free SBF. Reprinted from Burrows et al. (2004).

In addition to preventing barite sag, the System has provided other important field-documented performance advantages:

1. Whole mud losses reduced by an average of 60% while drilling, running casing, and cementing (with 80% reductions reported on several deep water wells).
2. Significantly lower ECDs, validated by pressure while drilling (PWD) data. As shown in Figure (2).
3. High, flat gel strengths that break with minimal initiation pressure, validated by

PWD data.

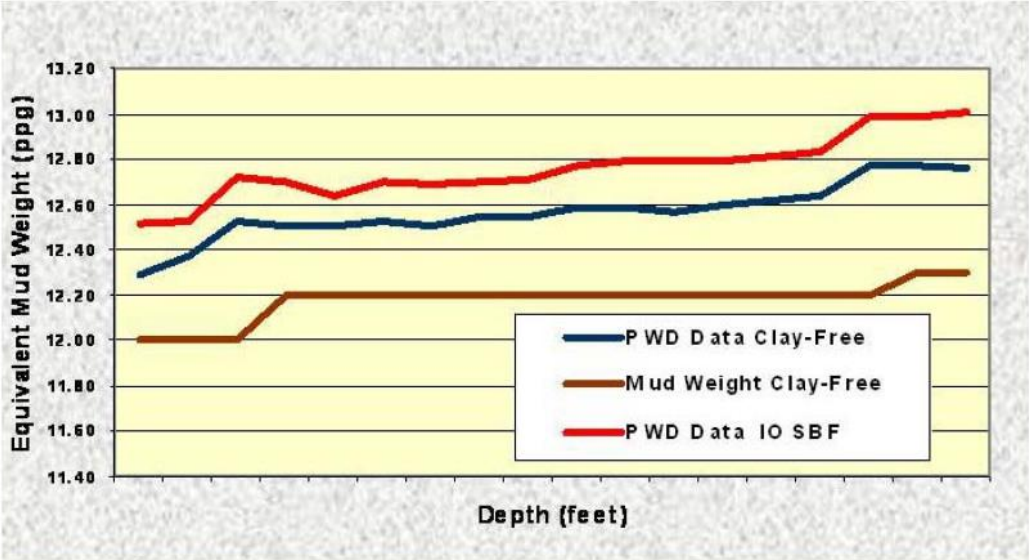

Figure 2. PWD comparison between System and conventional IO SBF during field trial. Reprinted from Burrows et al. (2004).

In 2016, Mahrous et al. (2016) documented the application of a high performance organo-clay-free invert-emulsion fluid (OCF-IEF) with low equivalent circulating density (ECD) characteristics to help drill well targets through depleted formations in the Carboniferous-aged Rotleigend reservoir formation in the North Sea, offshore Holland.

The successful trial application of the OCF-IEF allowed more challenging, longer step-outs, directional, and extended-reach drilling (ERD) wells to be drilled. The principal design concept was that the non-organophilic clay viscosifiers used in the formulation provided a flatter rheology profile over a full range of shear rates and a fragile thixotropic to the emulsion gel structure when fluid flow was initiated. These

features of the fluid resulted in the low ECD characteristics. Table 1 shows the fluid properties tracked from laboratory to field.

Table 1. Fluid properties tracked from laboratory to field. Reprinted from Mahrous et al. (2016).

Fluid Track	Formulation	Fluid Preparation	First Loadout	Sample Quality Check 1	Sample Quality Check 2	Offshore
	Lab	LMP	LMP	Lab		Rig
Fluid Properties	Confirmed Properties	Mixed Fluid Before Shearing With Shearing Unit	Mixed Fluid After Shearing With Shearing Unit	Before Hot Rolling	After Hot Rolling at 248°F	Fluid Checked Upon Arrival
Density	1.6	1.61	1.6	1.6	1.6	1.6
Θ 600	71	68	82	79	85	78
Θ 300	42	40	48	46	49	45
Θ 200	31	29	35	35	36	34
Θ 100	20	17	20	22	22	20
6-dial reading	6	4	5	6	6	5
3-dial reading	5	3	3	5	5	4
Plastic viscosity	29	28	34	33	36	33
Yield point	13	12	14	13	13	12
10-second gel	10	5	6	7	7	6
10-minute gel	19	9	14	23	18	13
30-minute gel	22	—	—	—	19	—
Tau 0	4.5	2.36	2.55	4.46	4.43	3.46

Despite the complexity of drilling the section, the fluids provider and operator managed to reach the top of the reservoir with the OCF-IEF system. Figure 3 shows an ECD comparison concluding a reduction of 7.5 to 8.6% (actual/planned) using the low ECD OCF-IEF system, versus 1.07% using conventional OBM. This drilling fluid system, with its success, allowed many of the future longer step-out, directional, ERD, and wellbore stability issues to be reduced during drilling operations of this magnitude.

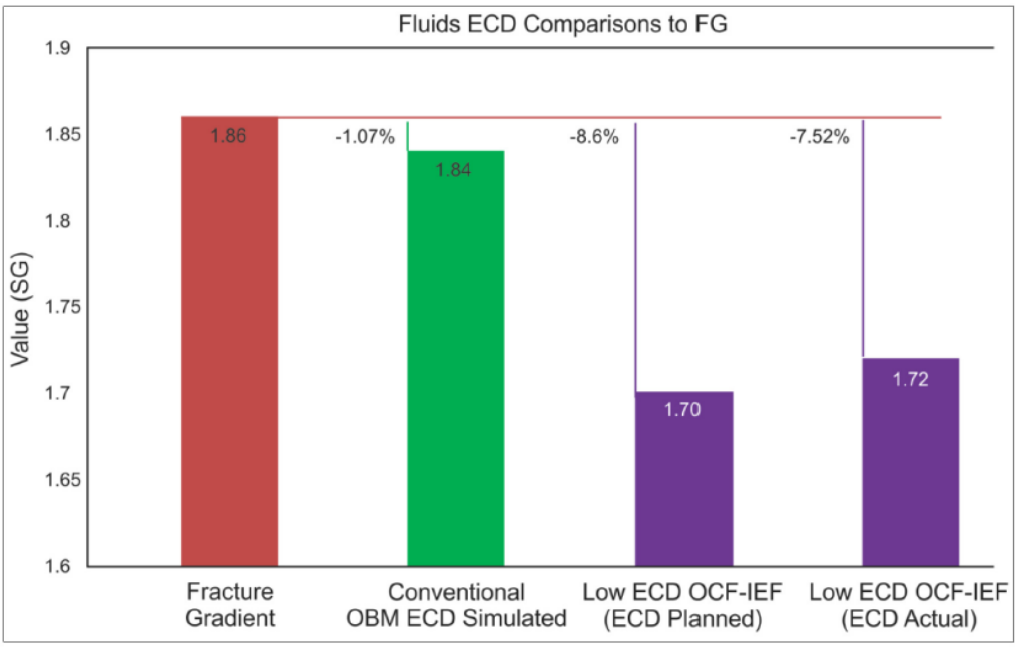

Figure 3. ECD comparisons conventional OBM vs. low ECD OCF-IEF to FG. Reprinted from Mahrous et al. (2016).

Ackal and Gillikin (2010) documented a seven-well development program in the Gulf of Mexico. The high-angle (54°-73°) 9-7/8" production intervals had shallow kick-off points (in one instance 70° by 3000 ft TVD, 30° average azimuth change, high of 67°). The complex well paths had proven difficult to drill with water-based fluids (WBF). Wellbore stability and torque and drag issues added to non-productive time (NPT). Previous wells drilled with WBF experienced slow penetration rates, multiple wiper trips, and one lost directional bottomhole assembly (BHA). The decision was made to use an organophilic clay-free synthetic-based fluid (SBF) on the seven-well project.

The clay-free SBF could run with a low synthetic oil-to-water ratio (SWR) in the range of 70/30 to 75/25 SWR as compared to the 80/20 SWR typically needed for conventional SBFs. Gels remained low and flat, even when the low gravity solids (LGS) content reached 15% on one well. The lower SWR values and reduced base oil dilution requirements helped keep fluid maintenance costs low. Shown in Figure 4.

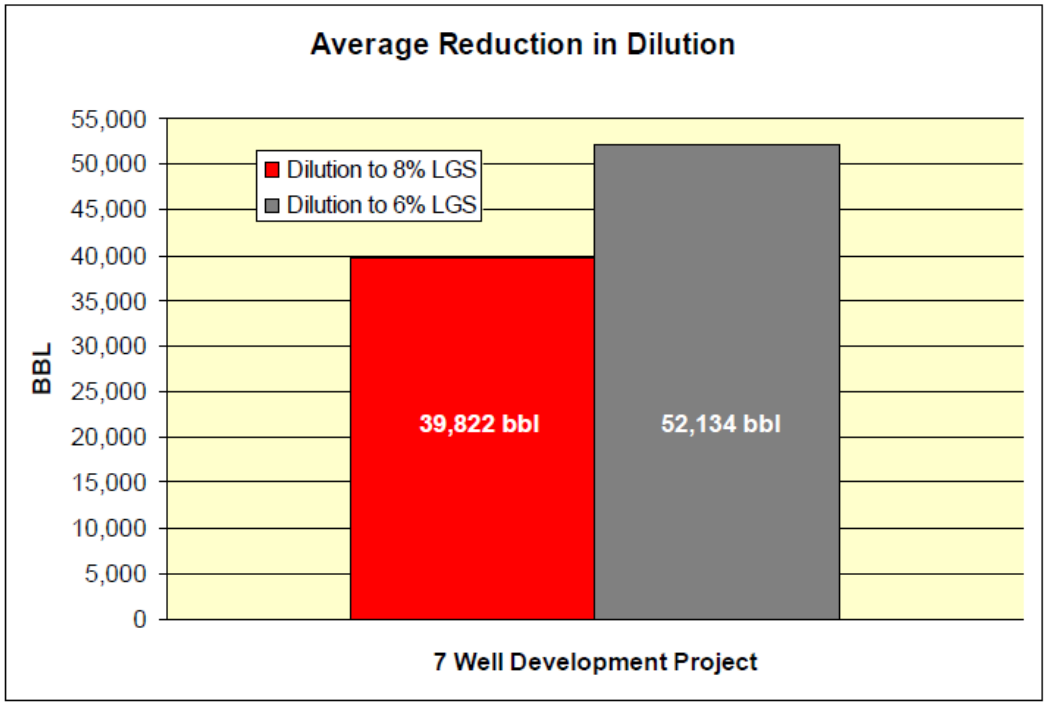

Figure 4. Using clay-free SBF with a low SWR significantly reduced base oil dilution requirements. Reprinted from Ackal and Gillikin (2010).

The use of the clay-free SBF allowed the operator to drill the wells considerably faster, at times drilling over 2,000 ft. per day despite the high percentage of LGS. No wellbore instability issues occurred, trips went smoothly and casing was run to bottom on every well. Four of the seven original wells reached total depth at 21% below

authority for expenditures (AFE) cost, and several sidetracks were drilled for geologic reasons using the same clay-free system.

The clay- free system provides the expected benefits of an SBF yet can be run with a lower SWR than a conventional clay-based SBF, reducing base oil requirements. The clay-free system selected for the development contained zero organophilic clay or lignite additives, so the solids content was inherently lower than that of conventional SBFs. The emulsion chemistry provided the yield point values and gel strengths required for good suspension and sag prevention, while exhibiting shear-thinning behavior for rapid gel-to-flow transitions when needed. ROPs were faster using the SBF, averaging almost double the ROP seen with WBF (Table 2).

Table 2. Average and Maximum Rates of Penetration. Reprinted from Ackal and Gillikin (2010).

Well - SBF	Avg ROP	High ROP
1	43.9'	86.0'
2	54.6'	67.5'
3	58.2'	97.3'
4	55.4'	93.9'
5	54.5'	98.4'
6	43.0'	76.4'
7	60.0'	94.4'
Well - WBF	Avg ROP	High ROP
1	21.6'	31.6'
2	32.4'	47.2'
3	27.7'	45.1'
4	27.3'	51.1'
5	36.5'	68.8'
6	27.8'	56.1'
7	18.9'	39.1'
8	27.1'	57.6'
9	31.1'	48.0'
Clay Free SBF AVG	**52.8'**	**87.7'**
WBF AVG	**27.8'**	**49.4'**

As previously mentioned, invert emulsion fluids require organophilic clays to provide viscosity and suspension characteristics. While effective, these drilling fluids are prone to stratification in certain conditions, slow chemical reaction times, high pressure spikes, and high ECDs.

Rødsjø and Akutsu (2013) described the first application of a clay-free IEFs in the Norwegian continental shelf. The clay-free IEF was used to drill into a section exhibiting temperatures greater than 160°C. Chemical consumption was substantially lower compared to previous wells using traditional IEF systems, thus reducing shipping

requirements. The polymer chemistry in the clay-free IEF provided a significant resistance to cold temperature and the rheology was significantly lower than those measured in conventional IEFs at low temperatures (e.g., 4^{o}C), an important observation for fluid viscosity in deep water marine risers.

Brookfield testing was performed on this fluid, as shown in Figure 5, and compared to traditional fluid to highlight the strength of the polymer interactions and their ability to break. Relative to other IEFs, clay-free IEFs exhibited a unique low end rheology signature, which deviated from conventional IEF systems at low shear rates. This demonstrates the increasingly formation of the strong gels as the shear rate is "stepped down" to low shear rates below 3 rev/min, and helps explain the excellent fluid stability observed in the field.

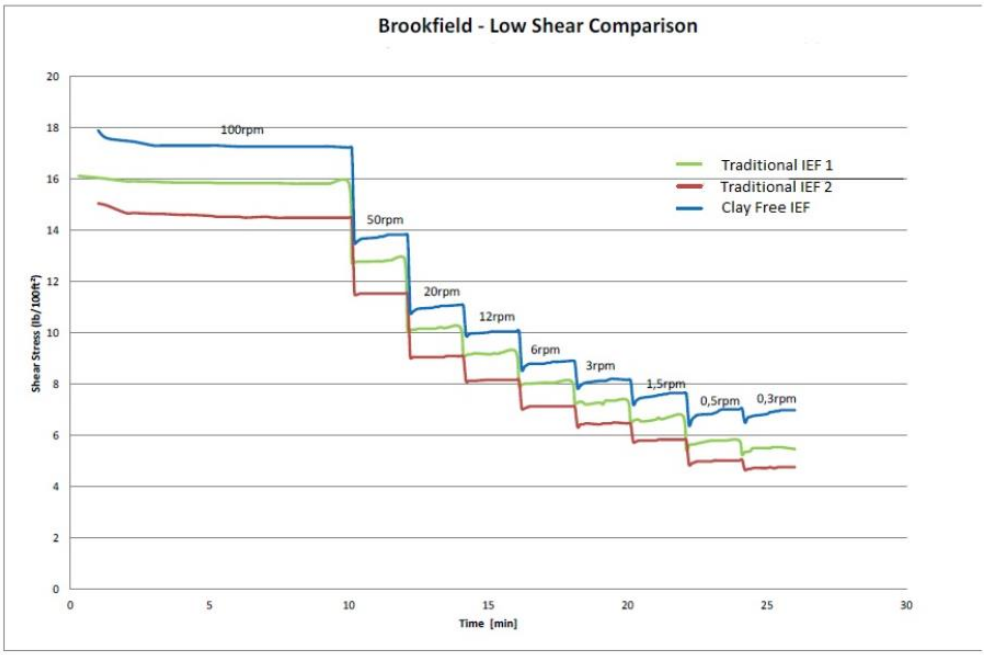

Figure 5. Brookfield testing on clay-free IEF compared to traditional IEF to highlight the strength of the polymer interactions and their ability to break. Reprinted from Rødsjø and Akutsu (2013).

When comparing the ECDs, it was clear that there was much better ECD control obtained with the clay-free IEF relative to the traditional organophilic clay-based IEF (Figs. 6 and 7). This comparison demonstrates the impact of increased ECDs recorded by the PWD downhole tools. The clay-free graph (Fig. 7) highlights that the ECD production was low enough not to induce losses.

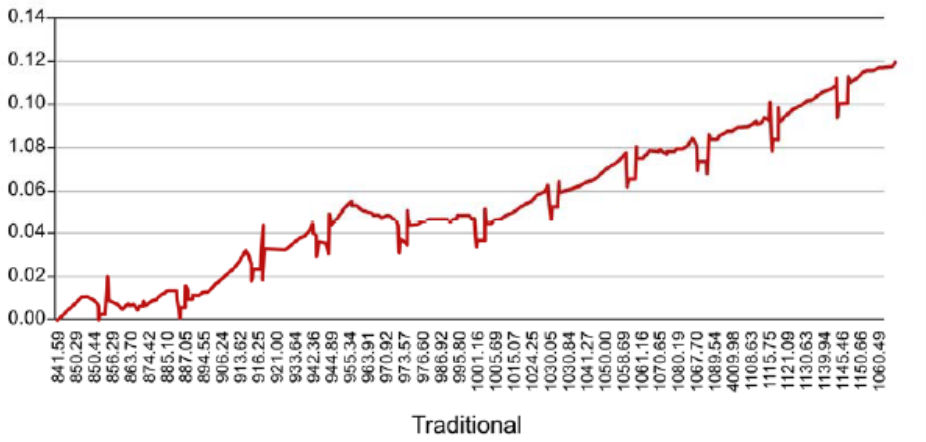

Figure 6. Increased ECD impact to the fluid density recorded on surface showing a much more progressive profile, increasing the potential for losses in this section. Reprinted from Rødsjø and Akutsu (2013).

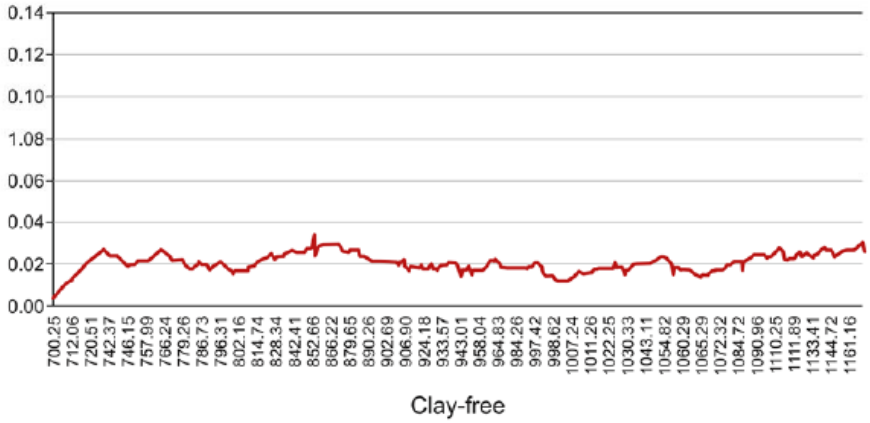

Figure 7. ECD impact to the fluid density recorded on surface. The ECD production was low enough not to induce losses. Reprinted from Rødsjø and Akutsu (2013).

The days versus depth curve shown in Figure 8 demonstrated a clear improvement compared to planned days. The well was placed in the 95th percentile of the Rushmore comparison, demonstrating that the well was drilled efficiently and safely.

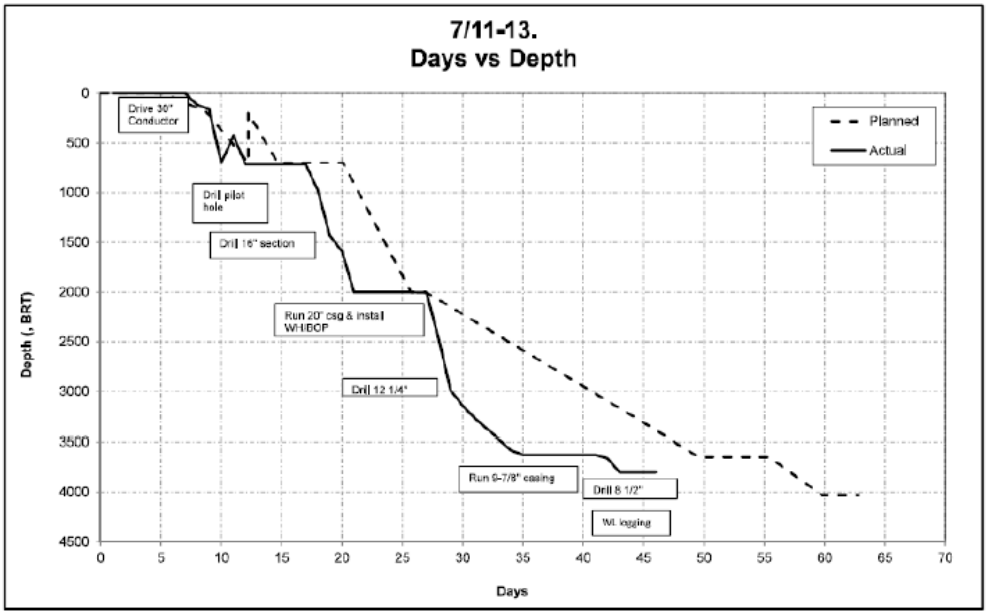

Figure 8. Days versus depth curve. Reprinted from Rødsjø and Akutsu (2013).

1.3 Research Objectives

The objectives of this work are:

1. Develop a novel mineral-oil-based drilling fluid (MOBDF) formula by replacing all organophilic clay additives with a novel polymer as a viscosifier and filtration control agent.
2. Evaluate the viscosity and suspension characteristics of the novel MODF and compare them to a MODF containing organophilic clay additives.

3. Evaluate the rheological, thermal stability, and filtration control properties of the novel MOBDF.
4. Evaluate the filter cake removal effectiveness of the novel MOBDF.
5. Determine if formation damage is caused by the novel MOBDF.

2. LITERATURE REVIEW

2.1 Fundamentals of Drilling Fluids

Drilling fluids are one of the most crucial elements of any drilling operation. The drilling fluid, or drilling mud, term used because of the thick consistency of the formulation, has several functions which all must be optimized to ensure safety and minimize hole problems.

In 1833 a French engineer named Flauville was watching a cable tool drilling operation in which the drilling apparatus struck water. He realized that the gushing water was very effective in lifting the cuttings out of the well. The principle of using moving fluid to remove cuttings from the well bore was established. He conceived of an assembly in which water would be pumped down the inside of a drilling rod and carry cuttings with it as it returned to the surface in the space between the drilling rod and the wall of the well bore. (Rabia 2001).

The early simple drilling fluids quickly gave way to increasingly “engineered” systems. To better protect the target formations, additives were developed for improved rheology and fluid-loss control, shale inhibition, and resistance to contamination. Laboratory and field-test procedures became more sophisticated as drilling-fluid companies and oil and gas operators sought correlations between surface measurements and downhole conditions. Under conditions in which bentonite and other clay additives proved inadequate, organic and synthetic polymers were substituted as viscosifiers and fluid-loss-control agents. (Mitchell and Miska 2011).

The success of the drilling operation strongly depends on the selection of the drilling fluid. Because drilling conditions vary widely, factors such as: the selection of the base liquid (the continuous fluid phase of the drilling mud), environmental restrictions, drill cuttings transport, interactions of the chemical additives with the formation, and the control of the drilling fluid properties must all be taken into consideration when selecting the proper drilling fluid formulation. But one thing is certain, no drilling fluid is suitable for all situations.

2.1.1 Types of Drilling Fluids

A drilling fluid can be classified by the nature of its continuous fluid phase and its constituents as shown in Figure 9. There are three types of drilling fluids:

1. Water-based drilling fluids.
2. Oil-based drilling fluids.
3. Gas-based (pneumatic) drilling fluids.

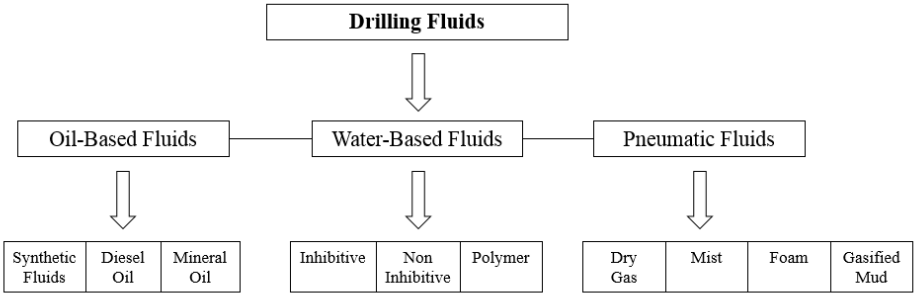

Figure 9. Drilling fluids classification by composition.

Fluids in general can be grouped into two according to their flow behavior: Newtonian and non-Newtonian. Figure 10 illustrates the two groupings with examples.

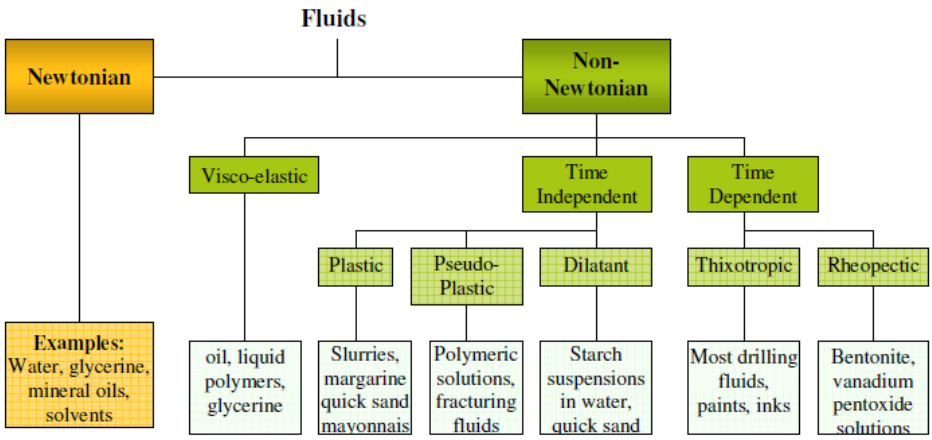

Figure 10. General fluid grouping by flow behavior. Reprinted from Ibeh (2007).

Water-Based Drilling Fluid (WBDF)

Water-based drilling fluids (WBDF) are the most common type of drilling fluids used in the industry. The base fluid may be fresh water, seawater, brine, saturated brine, or a formate brine. The type of fluid selected depends on anticipated well conditions or on the specific interval of the well being drilled.

Inhibitive fluids retard clay swelling. For this reason, inhibitive fluids are used for drilling hydratable-clay zones. Inhibitive fluid systems do not use chemical dispersants (thinners) or inhibitive ions, but native waters. They are designed to reduce chemical reactions between the drilling fluid and the formation. Fluid formulations containing sodium, calcium, and/or potassium ions to minimize shale hydration and swelling. Saltwater drilling fluids are used for shale inhibition and for drilling salt

formations. They are also known to inhibit hydrates (ice-like formations of gas and water) from forming, which can accumulate around subsea wellheads and well-control equipment, blocking lines and impeding critical operations. The mechanisms of inhibition vary according to the type of inhibitive product being used. It is common to utilize two or more products in the same mud system. These mud systems also minimize the reaction with the drilled cuttings and therefore help to avoid the high dilution rates exhibited by other fluid groups. (Mitchell and Miska 2011)

Non-Inhibitive fluids do not contain additives to inhibit downhole problems. They can be classified as non-dispersed and dispersed. Non-dispersed fluids do not do not contain inhibiting ions such as chloride (Cl^-), calcium (Ca_2^+) or potassium (K^+) in the continuous phase and do not utilize chemical thinners or dispersants to affect control of rheological properties. While dispersed fluids do not contain inhibiting ions in the continuous phase, but they do rely on thinners or dispersants such as phosphates, lignosulfonate or lignite to achieve control of the fluids' rheological properties. (Rabia 2001)

Polymer fluids may be inhibitive or non-inhibitive depending upon whether an inhibitive cation is used.

The density of the WBDFs can be increased by adding calcium carbonate particles. High levels of suspended solids, however, in drilling fluids can cause high frictional losses during fluid circulation. These loses create high Equivalent Circulating Densities (ECDs) and limit pump rates. Low pump rates can result in inefficient hole cleaning (Njobuenwu and Wobo, 2007).

The main concern with WBM is the thermal degradation of chemical additives that often occurs while drilling high temperature wells. Such degradation can lead to strong variations in rheological and filtration characteristics and loss of fluid properties (Melbouci and Sau Arjun, 2006).

A typical WBDF composition is shown in Figure 11.

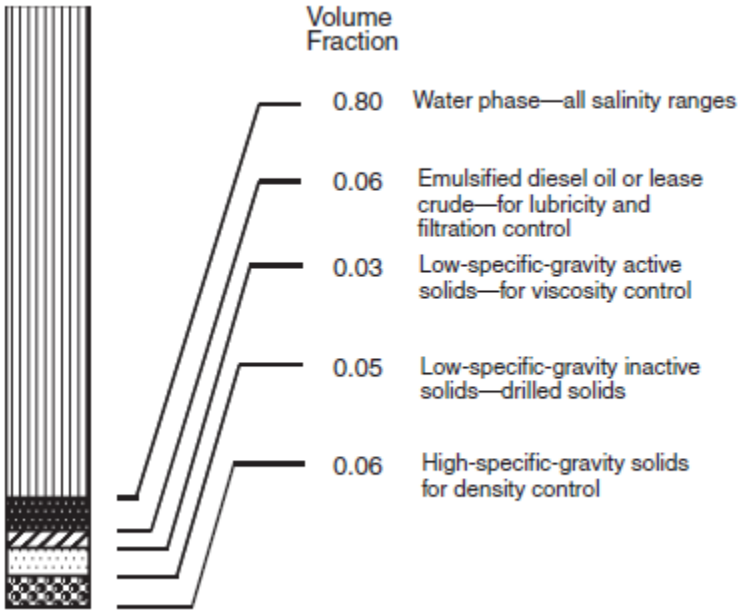

Figure 11. Composition of 11-lbm/gal water-based mud. Reprinted from Bourgoyne et al. (1991).

Oil-Based Drilling Fluid (OBDF)

An oil-based drilling fluid is one in which the continuous phase of a drilling fluid is oil. When water is added as the discontinuous phase then it is called an invert emulsion. The base fluids most often selected are diesel, mineral oil, and low-toxicity mineral oil. These fluids are particularly useful in drilling production zones, shales and other water-sensitive formations, as clays do not hydrate or swell in oil. OBDFs are also known to provide unequaled performance attributes with respect to the rate of penetration, wellbore stability, high lubricity, high thermal stability, and high salt tolerance. They are also useful in drilling high angle/horizontal wells because of their superior lubricating properties and low friction values between the steel and formation which result in reduced torque and drag (Payne 1997).

The oil/water ratios typically range from 90:10 to 60:40. Generally, the higher the percentage of water, the thicker the drilling fluid is. High salinity levels in the water phase dehydrate and harden reactive shales by imposing osmotic pressures.

OBDFs are more cost-effective and efficient than water muds in the following situations:

1. Shale stability
2. Temperature stability
3. Lubricity (Shah et al.2010)
4. Corrosion resistance
5. Stuck pipe prevention
6. Contamination

7. Fluid loss control
8. By using palm oil as an alternative of diesel can be more environmentally friendly (Shah et al. 2010)
9. Thin filter cake (De Stefano et al. 2012)
10. Resistant to salt, anhydrite, H_2S and CO_2. (Amani et al. 2012)

However, they are subjected to strict environmental regulation regarding their discharge and recycling. They are flammable and may contain compounds that cause the failure of rubber goods such as hoses, O-rings, gaskets and Blowout Preventer (BOP) elements. Oil-base muds (OBM) lack gel structure and are difficult to viscosify so they can be weighted.

A typical OBDF composition is shown in Figure 12.

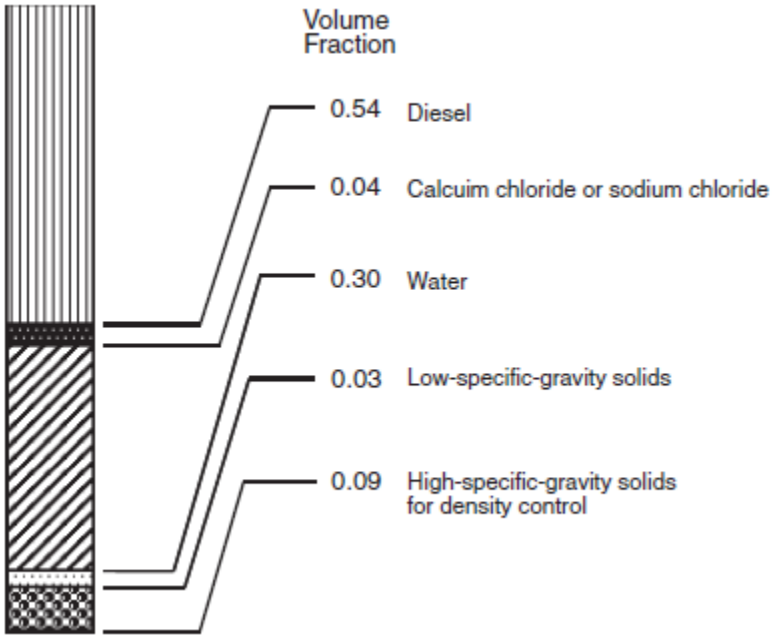

Figure 12. Composition of 11-lbm/gal oil-based mud. Reprinted from Bourgoyne et al. (1991).

Synthetic-based fluids (SBFs) were developed to provide the highly regarded drilling-performance characteristics of conventional OBFs while significantly reducing the toxicity of the base fluid. Consequently, SBFs are used almost universally offshore and they continue to meet the increasingly rigorous toxicity standards imposed by regulatory agencies. The cost-per-barrel for an SBF is considerably higher than that of an equivalent-density water-based fluid, but because synthetics facilitate high ROPs and minimize wellbore-instability problems, the overall well-construction costs are generally less, unless there is a catastrophic lost-circulation occurrence. (MI SWACO Engineering Manual 1998).

Gas-Based (Pneumatic) Drilling Fluid

These are not common systems as they have limited applications such as the drilling of depleted reservoirs or aquifers where normal mud weights would cause severe loss circulation. In the case of air, the maximum depth drillable is currently about 6-8,000 ft because of the capabilities of the available compressors (Mitchell and Miska 2011). Water if present in the formation is very detrimental to the use of gas-based muds as their properties tends to break down in the presence of water.

Gas or pneumatic drilling fluids are most commonly used in dry, hard formations such as limestone or dolomite. In pneumatic drilling-fluid systems, air compressors circulate air through the drillstring and up the annulus to a rotating head. The return "fluid" is then diverted by the rotating head to a flowline leading some distance from the

rig to protect personnel from the risk of explosion. (MI SWACO Engineering Manual 1998).

2.1.2 Rheology

The physical properties of a drilling fluid, density and rheological properties are monitored to assist in optimizing the drilling process. These physical properties contribute to several important aspects for successfully drilling a well, including:

1. Provide pressure control to prevent an influx of formation fluid.
2. Provide energy at the bit to maximize Rate of Penetration (ROP).
3. Provide wellbore stability through pressured or mechanically stressed zones.
4. Suspend cuttings and weight material during static periods.
5. Permit separation of drilled solids and gas at surface.
6. Remove cuttings from the well.

Overview

Rheology is the science of deformation and flow of matter. By making certain measurements on a fluid it is possible to determine how that fluid will flow under a variety of conditions, including temperature, pressure and shear rate.

The deformation of a fluid can simply be described by two parallel plates separated by some distance as shown in Figure 13.

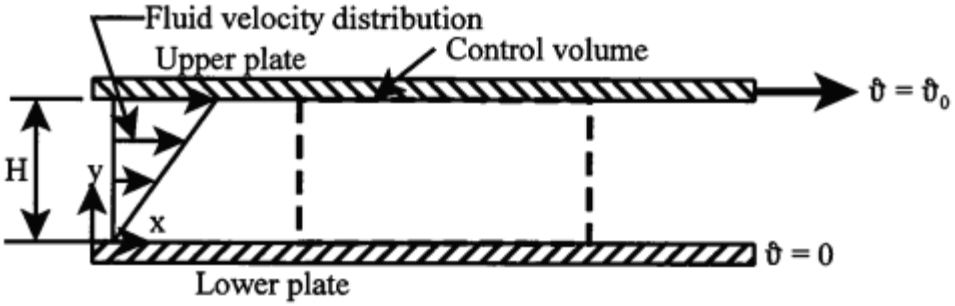

Figure 13. Deformation of a Fluid by Simple Shear. Reprinted from Rabia (2001).

Shear Stress

An applied force (F), acting over an area (A), causes the layers to slide past one another. However, there is a resistance, or frictional drag, force that opposes the movement of these plates. This resistance or drag force is called shear stress (τ). In equation form**,**

$$\tau = \frac{F}{A}, \qquad \text{..... (1)}$$

with shear stress having typical units of lbf/100 ft^2. Additionally, the fluid layers move past each other easier than between a pipe wall and fluid layer. Therefore, we can consider a very thin layer of fluid next to the pipe wall as stationary. (Baker Hughes Drilling Fluids Reference Manual 2006).

Shear Rate

The difference in the velocities between two layers of fluid divided by the distance between the two layers is called the shear rate (γ). In equation form,

$$\gamma = \frac{velocity\ diffrence}{distance} \quad \text{.....} \quad (2)$$

With typical units of

$$\frac{ft/sec}{ft} = \frac{1}{sec} = sec^{-1}$$

Newtonian and Non-Newtonian Fluids

The relationship between shear stress (τ) and shear rate (γ) defines the flow behavior of a fluid. For some fluids, the relationship is linear. Such fluids are called Newtonian fluids. Examples of Newtonian fluids include water, alcohols, and light oils. Very few drilling fluids fall into the Newtonian category. Fluids which have flow characteristics such that the shear stress does not increase in direct proportion to the shear rate are called non-Newtonian fluids. Most drilling fluids are of this type. (Baker Hughes Drilling Fluids Reference Manual 2006).

Viscosity

Of the rheological terms, viscosity is the most familiar. Is a measure of a fluid's resistance to flow. It describes the internal friction of a moving fluid. A fluid with large viscosity resists motion because its molecular makeup gives it a lot of internal friction. A fluid with low viscosity flows easily because its molecular makeup results in very little friction when it is in motion. (Mitchell and Miska 2011).

For a Newtonian fluid, the relationship between viscosity, shear stress and shear rate is defined as the viscosity (μ) of the fluid where:

$$\mu = \frac{\tau}{\gamma} \qquad \text{..... (3)}$$

For non-Newtonian fluids, the relationship between shear stress and shear rate is defined as the effective viscosity. However, the effective viscosity of a non-Newtonian fluid is not constant. For most drilling fluids, the effective viscosity will be relatively high at low-shear rates, and relatively low at high-shear rates. In other words, the effective viscosity decreases as the shear rate increases. When a fluid behaves in this manner, it is said to be shear thinning. Shear thinning is a very desirable characteristic for drilling fluids. (Baker Hughes Drilling Fluids Reference Manual 2006).

As shown in Figure 14, when the effective viscosity is plotted alongside the shear-stress-shear-rate curve, it is easy to see the shear-thinning nature that most drilling fluids exhibit. Shear thinning has very important implications in drilling fluids as it provides what we desire most:

1. At high velocities (high shear rates) in the drillstring and through the bit, the mud shear thins to low effective viscosities. This reduces the circulating pressure and pressure losses.
2. At the lower velocities (lower shear rates) in the annulus, the mud has a higher effective viscosity that aids in hole cleaning.
3. At ultra-low velocity the mud has its highest effective viscosity and when not circulating will develop gel strengths that aid in suspending weight material and

cuttings. (MI SWACO Engineering Manual 1998).

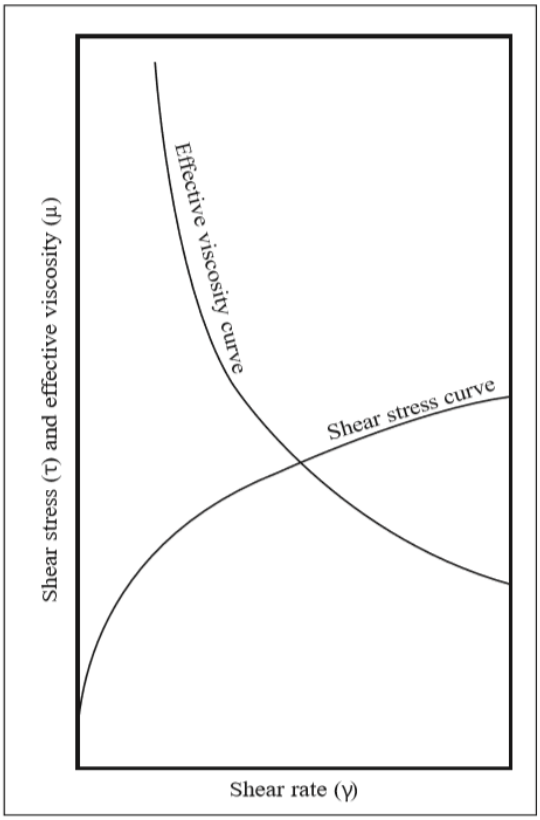

Figure 14. Shear-thinning effect in Non-Newtonian fluids. Reprinted from MI SWACO Engineering Manual (1998).

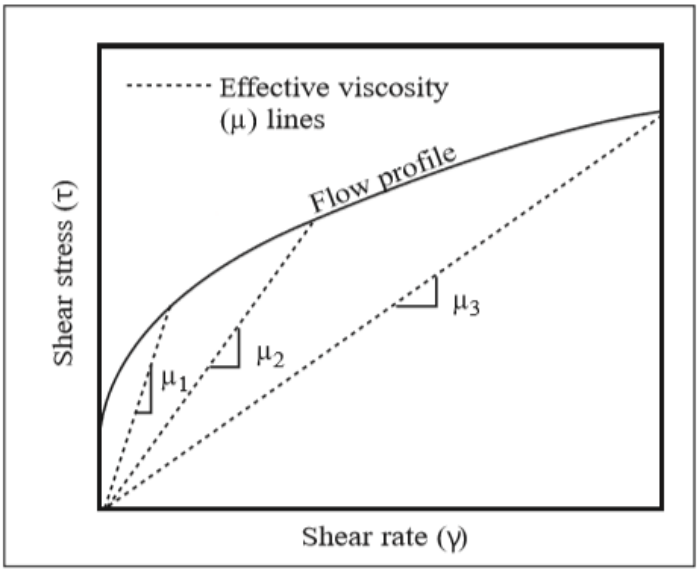

Figure 15. Effect of shear rate on effective viscosity of Non-Newtonian fluid. Reprinted from MI SWACO Engineering Manual (1998).

Dynamic Viscosity

The dynamic viscosity of a fluid expresses its resistance to shearing flows, where adjacent layers move parallel to each other with different speeds. It can be defined through the idealized situation known as a Couette flow, where a layer of fluid is trapped between two horizontal plates, one fixed and one moving horizontally at constant speed u. This fluid has to be homogeneous in the layer and at different shear stresses. (The plates are assumed to be very large so that one need not consider what happens near their edges.). (MI SWACO Engineering Manual 1998).

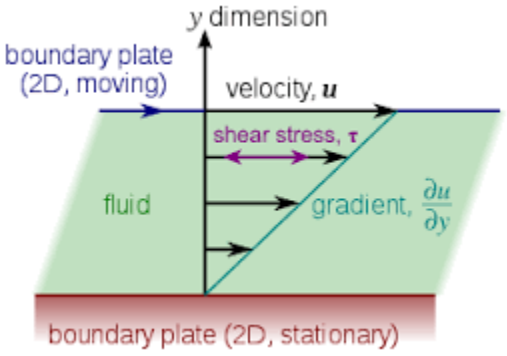

Figure 16. Two-Plates-Model of viscosity. Reprinted from Quora.com

Kinematic Viscosity

Defined as the dynamic viscosity divided by the density of the material. This results in units with dimensions of area per unit of time. When the units are mm2/s they are known as centistokes (cSt).

$$\nu = \frac{\mu}{\rho} \qquad \text{..... (4)}$$

2.1.3 Rheological Models

A rheological model is a description of the relationship between the shear stress and shear rate. Newton's law of viscosity is the rheological model describing the flow behavior of Newtonian fluids. It is also called the Newtonian model. However, since most drilling fluids are non-Newtonian fluids, this model does not describe their flow behavior. In fact, since no single rheological model can precisely describe the flow characteristics of all drilling fluids, many models have been developed to describe the flow behavior of non-Newtonian fluids. (MI SWACO Engineering Manual 1998).

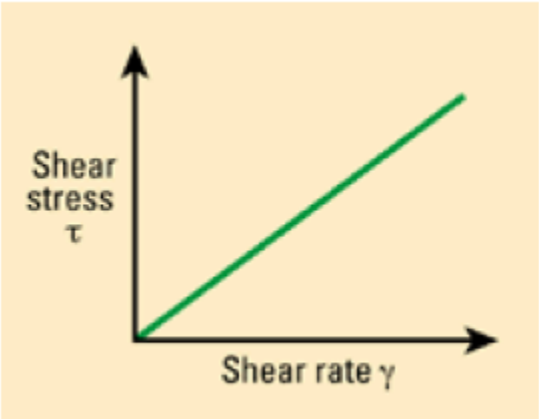

Figure 17. Shear stress vs. shear rate for a Newtonian Fluid. Reprinted from Baker Hughes Drilling Fluids Reference Manual (2006).

Bingham Plastic Model

The Bingham Plastic model has been used most often to describe the flow characteristics of drilling fluids. It is one of the older rheological models currently in use. The Bingham Plastic model (Bingham 1922) is defined by:

$$\tau = (\mu_p)(\gamma) + \tau_o \qquad \text{.....} \quad (5)$$

Where,

τ = shear stress

τ_o = yield point

μ_p = plastic viscosity

γ = shear rate.

$\tau > \tau_o$

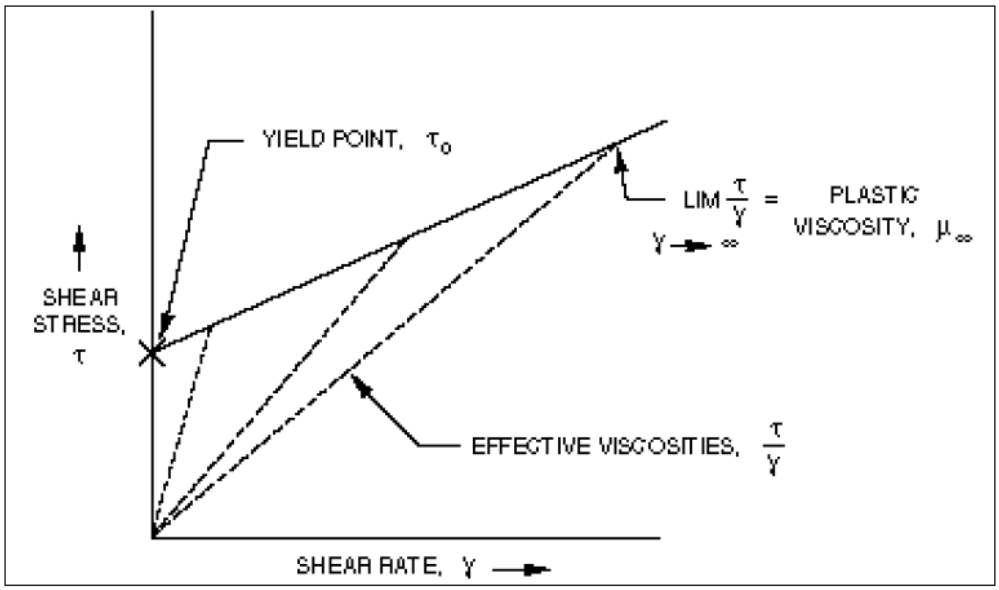

Figure 18. Shear stress vs. shear rate for a Bingham plastic fluid. Reprinted from Baker Hughes Drilling Fluids Reference Manual (2006).

No bulk movement of the fluid occurs until the applied force exceeds the yield stress. The yield stress is commonly referred to as the Yield Point (YP). In Bingham Plastic model a fluid will flow if the shear stress τ is greater than YP. Shear stress is proportional to shear rate, this ratio is called plastic viscosity (PV), μ_p . YP typically is shown in field units of lbf/100 ft^2. (MI SWACO Engineering Manual 1998).

The effective viscosity is visually represented by the slope of a line from the origin to the shear stress at some particular shear rate as shown in Figure 18. The slopes of the dashed lines represent effective viscosity at various shear rates. As can be seen, the effective viscosity decreases with increased shear rate. Plastic viscosity is used as an indicator of the size, shape,

distribution and quantity of solids, and the viscosity of the liquid phase. The yield point is a measure of electrical attractive forces in the drilling fluid under flowing conditions. (Shah et al. 2010).

Power Law Model

Most drilling fluids exhibit behavior that falls between the behaviors described by the Newtonian Model and the Bingham Plastic Model. This behavior is classified as pseudo plastic. The relationship between shear stress and shear rate for pseudo plastic fluids is defined by the power law mathematical model,

$$\tau = K(\gamma^n) \qquad \text{.....} \quad (6)$$

where,

τ = shear stress

K = consistency factor

n = flow behavior index

γ = shear rate.

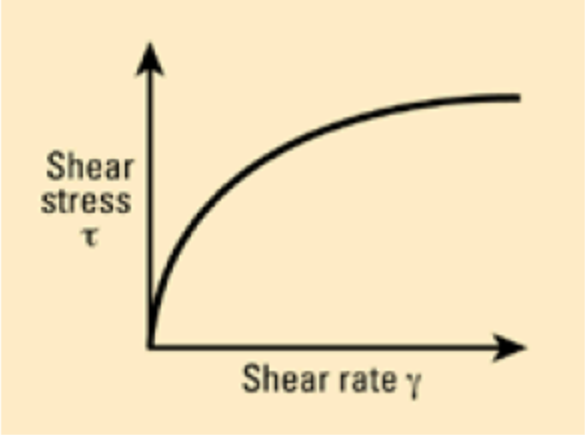

Figure 19. Shear stress vs. shear rate for a Power Law Fluid. Reprinted from Baker Hughes Drilling Fluids Reference Manual (2006).

The two terms, K and n, are constants in the Power Law Model. Generally, K is called the consistency factor and describes the thickness of the fluid and is thus somewhat analogous to effective viscosity. If the drilling fluid becomes more viscous, then the constant K must increase to adequately describe the shear stress/shear rate relationship. (MI SWACO Engineering Manual 1998).

Additionally, n is called the flow behavior index and indicates the degree of non-Newtonian behavior. A special fluid exists when n = 1, when the Power Law Model is identical to the Newtonian Model. If n is greater than 1, another type of fluid exists classified as dilatant, where the effective viscosity increases as shear rate increases. For drilling fluids, the pseudo plastic behavior is applicable and is characterized when n is between zero and one. Pseudo plastic fluids exhibit shear thinning, where the effective viscosity decreases as the shear rate increases just like the Bingham Plastic Model. (Shah et al. 2010).

Herschel-Bulkey Model

The Herschel-Bulkley model (Herschel and Bulkley 1926) is defined by

$$\tau = \tau_y + K\dot{\gamma}^n \quad \text{……...……..……} \quad (7)$$

Where,

τ = shear stress

τ_y = yield point

K = consistency factor

n = flow behavior index

$\dot{\gamma}$ = shear rate.

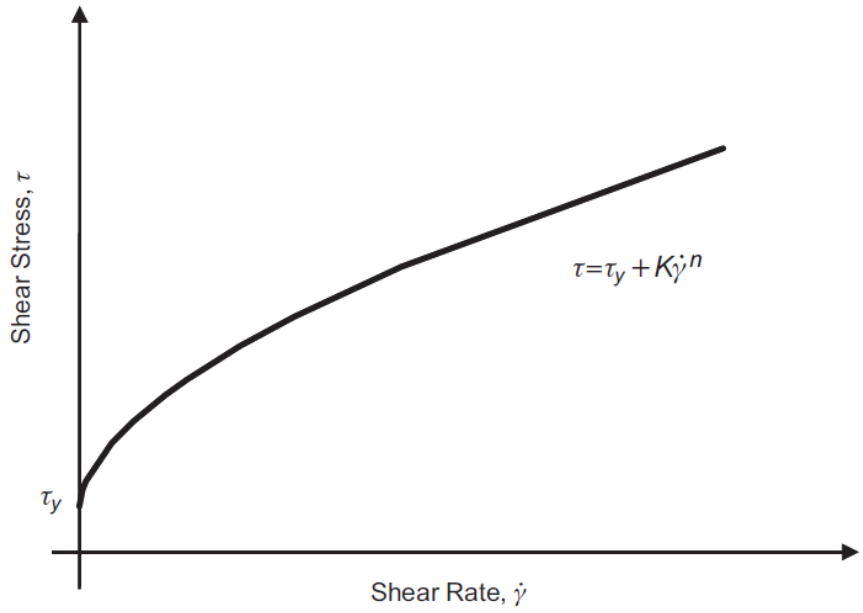

Figure 20. Shear stress vs. shear rate for a Herschel-Bulkley Fluid. Reprinted from Mitchell and Miska (2011).

The Herschel-Bulkley Model is a Power Law Model that includes a yield stress parameter. Requires 3 parameters for fluid characterization. The model can be used to represent a pseudoplastic fluid if *n* is less than 1, a dilatant fluid if *n* is equal to 1, a pseudoplastic fluid if τ_y is equal to 0, and *n* is less than 1, a plastic fluid if *n* is equal to 1, or a Newtonian fluid if τ_y is equal to 0, and *n* is equal to 1. The model fits OBDF and SBF across an extensive variety of pressures, temperatures and shear rates. The Helschel-Bulkley model is more widely used than previously as it is seen to more accurately describe most fluids than the simpler Power Law and Bingham models. (Baker Hughes Reference Manual 2006).

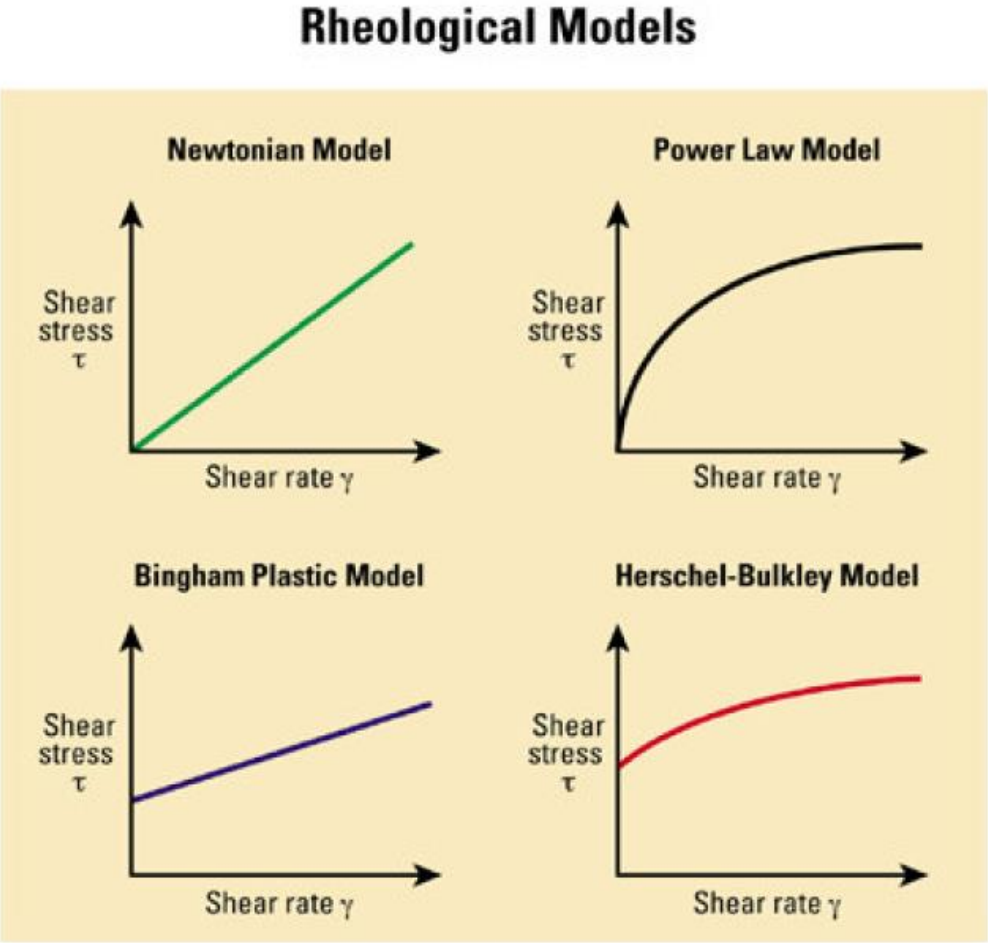

Figure 21. Shear stress versus shear rate for various rheological models. Reprinted from Baker Hughes Drilling Fluids Reference Manual (2006).

2.2 Functions of Drilling Fluids

Baker Hughes, in their Drilling Fluids Reference Manual, presented a thorough analysis of the functions of the drilling fluids. Among these functions, the most important include:

1. Transport cuttings: Drilling fluids transport cuttings from the well bore as drilling progresses. Many factors influence the removal of cuttings from the hole.

   The velocity at which fluid travels up the annulus is the most important hole cleaning factor. The annular velocity must be greater than the slip velocity of the cuttings for the cuttings to move up the wellbore.

   The size, shape, and weight of a cutting determine the viscosity necessary to control its settling rate through a moving fluid. Low shear rate viscosity strongly influences the carrying capacity of the fluid and reflects the conditions most like those in the well bore. The drilling fluid must have sufficient carrying capacity to remove cuttings from the hole.

   The density of the suspending fluid has an associated buoyancy effect on the cuttings. An increase in density increases the capacity of the fluid to carry cuttings.

2. Chemical Stability: Chemical interactions between the exposed formations of the borehole and the drilling fluid are a major factor in borehole stability. Isolating the fluid from the formation minimizes the potentially detrimental interaction between the filtrate and the formation. This is accomplished by controlling mud

filtrate invasion of the formation. Filtrate invasion may be controlled by the type and quantity of colloidal material and by filtration control materials and special additives in the drilling fluid

3. Control bottom hole pressure: As the formation pressure increases, the density of the drilling fluid is increased to balance or slightly overbalance the well and keep it in control. As drilling progresses, oil, water, or gas may be encountered. Sufficient hydrostatic pressure must be exerted by the drilling fluid column to prevent influx of these fluids into the borehole. The amount of hydrostatic pressure depends on the density of the fluid and the height of the fluid column, i.e., well depth.
4. Cool and lubricate the bit and drillstring: Considerable heat is generated by rotation of the bit and drillstring. The drilling fluid acts as a conductor to carry this heat away from the bit and to the surface. Current trends toward deeper and hotter holes make this a more important function.

   The drilling fluid also provides lubrication for the cutting surfaces of the bit thereby extending their useful life and enhancing bit performance.

   Filter cake deposited by the drilling fluid provides lubricity to the drill string, as do various specialty products. Oil and synthetic base fluids are lubricious by nature.
5. Provide buoyancy for the drillstring: The drilling fluid helps to support a portion of the drillstring or casing string weight through buoyancy.

6. Suspend cuttings/weighting material when circulation ceases: When circulation is stopped, drilling fluids must suspend the drilled cuttings and weight material. Circulation of the suspended material continues when drilling resumes. The drilling fluid should also exhibit properties which promote efficient removal of solids by surface equipment.
7. Facilitate the retrieval of information from the wellbore: Obtaining maximum information on the formation being penetrated is imperative. A fluid which promotes cutting integrity is highly desirable for evaluation purposes. The use of electronic devices incorporated within the drill string has made logging and drilling simultaneous activities.
8. Limit corrosion of drillstring, casing, and tubular goods: Corrosion in drilling fluids is usually the result of contamination by carbon dioxide, hydrogen sulfide, oxygen or, in the case of static fluids, bacterial action. Low pH, salt-contaminated, and non-dispersed drilling fluids are inherently more corrosive than organically treated freshwater systems. Oil or synthetic-based fluids are considered non-corrosive. A proper drilling fluid corrosion control program should minimize contamination and render the contaminating source non-corrosive
9. Transmit hydraulic energy to the tools and bit: Once the bit has created a drill cutting, this cutting must be removed from under the bit. If the cutting remains, it will be “re-drilled” into smaller particles which adversely affect penetration rate of the bit and fluid properties. The drilling fluid serves as the medium to remove

these drilled cuttings. One measure of cuttings removal force is hydraulic horsepower available at the bit. Fluid density and viscosity affect bit hydraulic horsepower.

2.3 Composition of Oil-Based Drilling Fluids

1. Mineral Oil: Mineral oils have lower aromatic (<1.0%) content than diesel and are also considered less toxic. They have higher flash points than diesel and are safer to use especially in high temperature applications. Also, they have a low viscosity when compared to diesel and crude oils which will affect the overall viscosity of the oil-based mud. Unlike diesel, mineral oils do not contain surfactants that could change the wettability of the formation.
2. Emulsifiers: Are surfactants that reduce the surface tension between the water droplets and oil which allows stable emulsions with small drops to be formed. They are amphiphilic compounds with both hydrophilic “heads” and organophilic “tails,” partially soluble in both water and oil. Historically, oil-mud emulsifiers have been classified as primary and secondary.

   Primary emulsifiers are used to reduce interfacial tension between the liquid phases and make the internal phase dispersible while secondary emulsifiers are very powerful oil wetting chemicals. Generally, these products do not form emulsions as well as the primary emulsifiers, they are used to emulsify any water intrusions quickly and stabilize the emulsion. Secondary emulsifiers consolidate stability of the dispersed phase. Fatty acids are the basic components for nearly

all emulsifiers and wetting agents used in the preparation of invert emulsions. Emulsifiers can be calcium fatty-acid soaps made from various fatty acids and lime, or derivatives such as amides, amines, amidoamines, and imidazolines made by reactions of fatty acids and various ethanolamine compounds.

3. Wetting agents: Is a surface-active agent that reduces the interfacial tension and contact angle between a liquid and a solid. This causes the liquid to spread over the surface of the solid.
4. Weighting material: Are compounds that are dissolved or suspended in drilling fluid to increase its density. They are used to control formation pressures and to help combat the effects of sloughing or heaving shales that may be encountered in stressed areas.
5. Soluble salts: Are used primarily to increase the fluid's density. Soluble salts are added to increase the emulsified water phase's salinity to provide inhibition of shales and reactive solids. Control of salinity in invert oil muds is necessary to "tie-up" free water molecules, and it prevents any water migration between the mud and the open formation such as in shales.
6. Viscosifiers: Primary function is to provide viscosity and improve the drilling fluid's ability to remove cuttings from the wellbore by producing high YP/PV ratios and gel strengths.
7. Filtration control materials: Reduce the amount of filtrate lost from the drilling fluid into a subsurface formation.
8. Rheology control material: Materials called thinners, dispersants, or

deflocculants that are used to improve/control the rheology of the fluid. These materials reduce the viscous and structure-forming properties of the drilling fluid by changing the physical and chemical interactions between solids and/or dissolved salts.

2.4 Rheology Properties and Filtration Control of Oil-Based Drilling Fluids

As previously discussed, the rheology properties of a drilling fluid contribute to several important aspects for successfully drilling a well. Among these are:

1. Provide pressure control to prevent an influx of formation fluid.
2. Provide energy at the bit to maximize ROP.
3. Provide wellbore stability through pressured or mechanically stressed zones.
4. Suspend cuttings and weight material during static periods.
5. Permit separation of drilled solids and gas at surface.
6. Remove cuttings from the well.

2.4.1 Funnel Viscosity

Funnel viscosity is used as a relative indicator of fluid condition. It does not provide sufficient information to determine the rheological properties or flow characteristics of a fluid. It should be used in the field to detect relative changes in the fluid's properties. The funnel viscosity is measured using the Marsh funnel. (MI SWACO Engineering Manual 1998).

2.4.2 Apparent viscosity (AV)

The viscosity of a non-Newtonian fluid changes with shear. The effective viscosity (μ_e) of a fluid is a fluid's viscosity under specific conditions. These conditions include shear rate, pressure and temperature. (MI SWACO Engineering Manual 1998).

2.4.3 Effective viscosity

The effective viscosity is sometimes referred to as the Apparent Viscosity (AV). The apparent viscosity is reported as either the mud viscometer reading at 300 RPM (Θ_{300}) or one-half of the meter reading at 600 RPM (Θ_{600}). (MI SWACO Engineering Manual 1998).

2.4.4 Plastic Viscosity (PV)

The plastic viscosity is the shear stress in excess of the yield stress that will induce a unit rate of shear. In other words, it is that part of the flow resistance in a drilling fluid mainly produced by the friction of the suspended particles and by the viscosity of the liquid phase. (MI SWACO Engineering Manual 1998).

When using the viscometer, the plastic viscosity in centipoise (cP) or milliPascal seconds (mPa•s) is found by subtracting the 300 RPM (Θ_{300}) reading from the 600 RPM (Θ_{600}) reading

$$PV = \Theta_{300} - \Theta_{600} \quad \text{..... (8)}$$

2.4.5 Yield Point (YP)

Yield point, the second component of resistance to flow in a drilling fluid, is a measurement of the electro-chemical or attractive forces in a fluid. These forces are a result of negative and positive charges located on or near the particle surfaces. Yield point is often used as an indicator of the shear thinning characteristics of drilling fluid and its ability to suspend cuttings and weight material. Yield point in pounds per 100 square feet (lb/100 ft^2) or in Pascals is calculated from the viscometer readings as:

$$YP\ \left({}^{lb}/_{100\ ft^2}\right) = 2\ x\ \Theta_{300} - \Theta_{600} \quad \ldots\ldots\ldots\ldots\ldots\ldots\ldots\ldots\ldots\ldots\ldots\ldots\ (9)$$

$$YP\ \left({}^{lb}/_{100\ ft^2}\right) = \Theta_{300} - PV \quad \ldots\ldots\ldots\ldots\ldots\ldots\ldots\ldots\ldots\ldots\ldots\ldots\ (10)$$

$$YP\ (Pa) = 0.4788\ x\ (2\ x\ \Theta_{300} - \Theta_{600}) \quad \ldots\ldots\ldots\ldots\ldots\ldots\ldots\ldots\ldots\ldots\ (11)$$

$$YP\ (Pa) = 0.4788\ x\ (\Theta_{300} - PV) \quad \ldots\ldots\ldots\ldots\ldots\ldots\ldots\ldots\ldots\ldots\ (12)$$

2.4.6 Gel Strength

Gel strength is a rheological parameter commonly used to describe non-Newtonian fluids. The gel strength is the shear stress measured at low shear rate after a mud has set quiescently for a period of time. In other words, it is the measure of ability of a colloidal solid at rest to form a gel. A colloid is a finely divided solid that does not deposit by gravity when dispersed in a liquid medium. Excessive gelation is caused by high solids concentrations leading to flocculation. There are two readings for gel

strengths, 10-second and 10-minute with the speed of the viscometer set at 3 rpm. The fluid must have remained static prior to each test, and the highest peak reading will be reported. (Xie 2001).

Signs of rheological trouble in a mud system often are reflected by the gel strength development of a mud with time shown in Figure 22. When there is a wide range between the initial and 10-minute gel readings they are called “progressive gels”. This is not a desirable situation. If the initial and 10-minute gels are both high, with no appreciable difference in the two, these are “high-flat gels”, also undesirable. Gelation should not be allowed to become much higher than is necessary to perform the function of suspension of cuttings and weight material. For suspension “low-flat gels” are desirable. (Xie 2001).

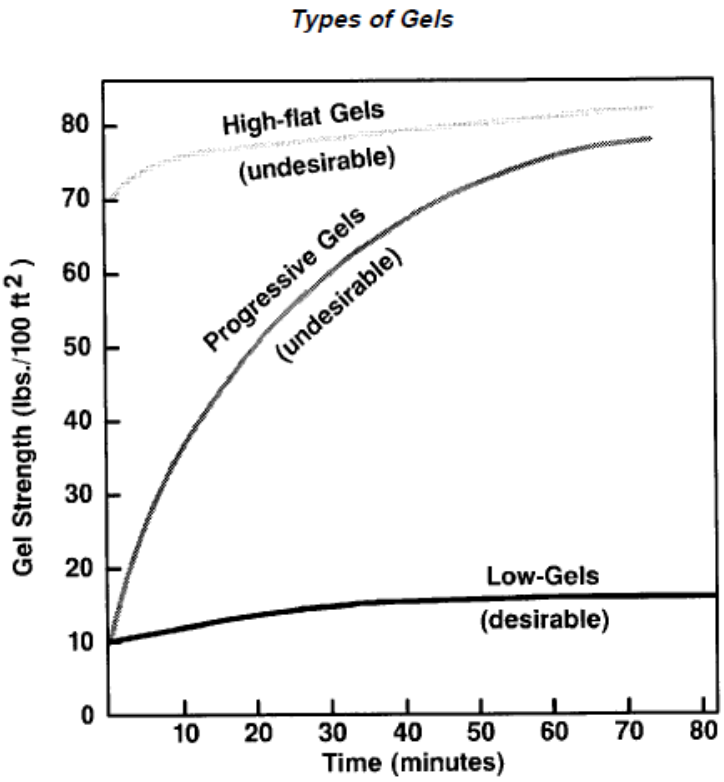

Figure 22. Different types of gel strengths. Reprinted from Xie (2001).

2.4.7 Filtration Control

Filtration process may occur under static or dynamic conditions. Static filtration occurs when the slurry is applied to a filter cake without cross-flow. Therefore, the particles are continuously deposited to form thicker filter cakes until the space available is full of the filter cake. Dynamic filtration involves cross-flow through the filter cake, which leads to variation in the thickness until the particle deposition and erosion rates become equal (Civan 1998).

At early stages of filtration, both large and small particles deposit on the cake surface; because the drag force driving the particles to the cake surface is high, then only

smaller and smaller particles are deposited (Jiao and Sharma 1994). The cake growth rate gradually decreases until an equilibrium filtration rate is attained at which no particles small enough to be deposited are available in the suspension. This mechanism of cake growth gives rise to a heterogeneous cake with both large and small particles at the internal and only small particles at the external portion of the cake.

Permeability of filter cake is controlled by the downhole static and dynamic filtration behavior of the drilling fluid. Thick filter cakes which have high permeability cause various operational problems such as excessive torque, drag, high swab and surge pressures, and sticking of pipes. There are many approaches used to determine the filter cake permeability. They assumed homogenous filter cake with constant properties of the filter medium.

3. MATERIALS, LABORATORY EQUIPMENT, AND METHODOLOGY

3.1 Materials

3.1.1 Cores and Minerology

High permeability Indiana limestone cores with a thickness of 0.25 in. and a diameter of 2.5 in. were used to perform the filter cake formation and filtration analysis. The properties of the cores and their mineralogy are shown in Tables 3 and 4.

Table 3. Properties of the Indiana Limestone cores.

Properties of the Indiana Limestone Cores	
Porosity, vol%	23 - 30
Permeability, md	100
Length, in	0.25
Diameter, in	2.5

Table 4. Minerology of the Indiana Limestone cores.

Mineral	**Concentration (wt%)**
Calcium carbonate	98
Quartz	1-2

Figure 23. Indiana Limestone core.

3.1.2 Oil-Based Drilling Fluid Formulas

Calcium carbonate ($CaCo_3$) was chosen as the weighting material for the two mineral-oil based drilling fluids used for the analysis. The properties if the weighting material are shown in Table 5. The first of the drilling fluids (MOBDF A) was prepared with a formula containing organophilic clay additives. The second fluid, a clay-free drilling fluid (MOBDF B), was prepared with a formula containing the replacement polymer viscosifier and filtration control agent. A complete list of the additives, the quantities used, and their respective mixing times are shown in Table 8 and Table 9.

The chemical additives used in this work such as viscosifiers, emulsifiers and fluid loss agents were supplied by the companies Baker Hughes and Halliburton.

Table 5. Properties of the Weighting Material.

Weighting Material	**Chemical Formula**	**Density, g/cm^3**	**D50, μm**	**Acid solubility**	**Mohs Hardness**
Calcium Carbonate	$CaCO_3$	2.8	50 - 55	Soluble	3 - 4

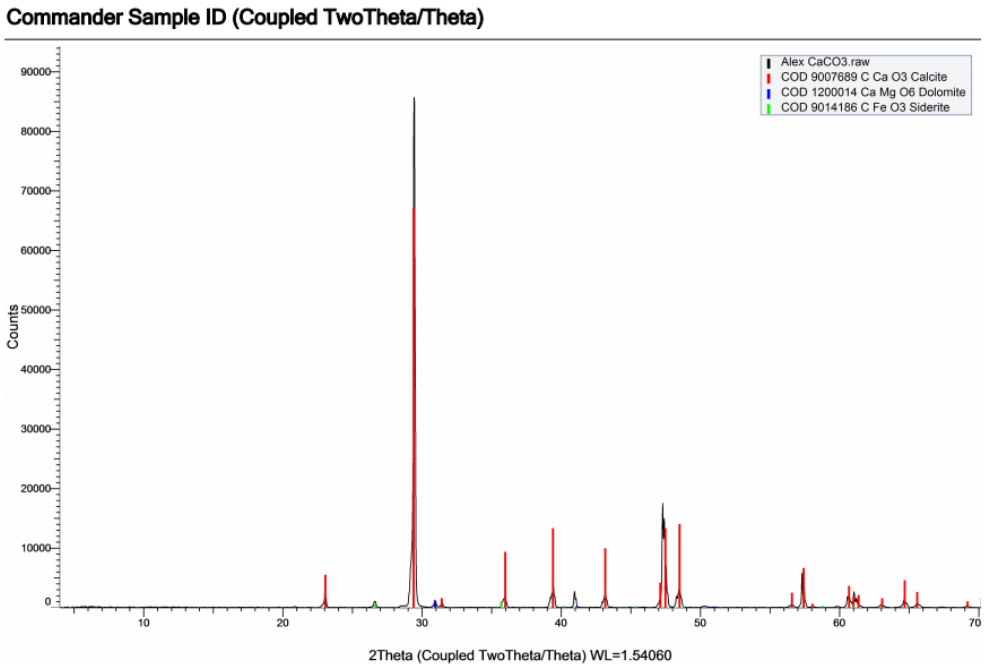

Figure 24. X-ray diffraction spectrum of the weighting material ($CaCO_3$) sample.

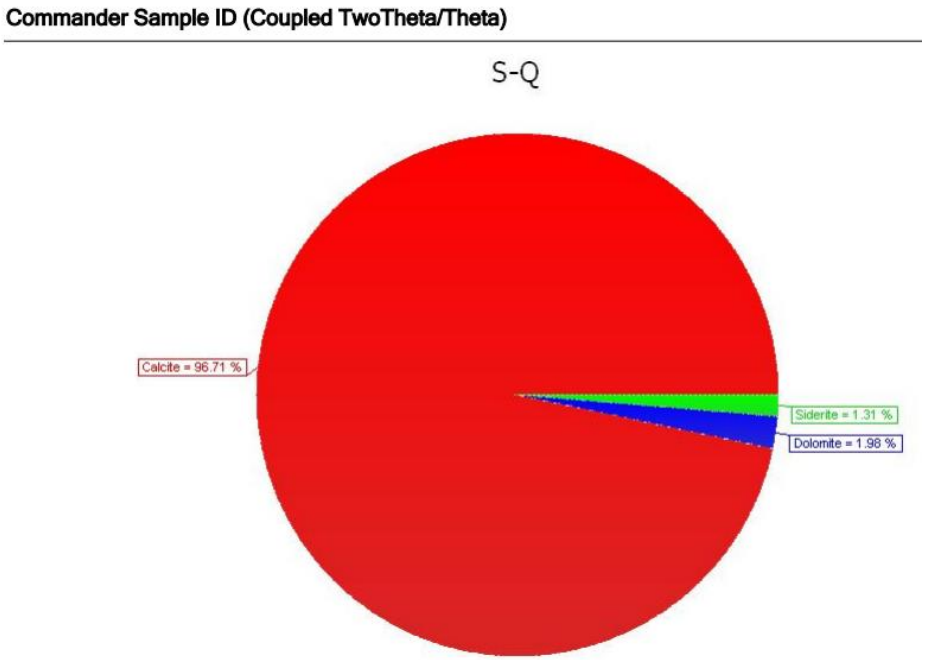

Figure 25. Compositon of the weighting material ($CaCO_3$) sample.

Table 6. Properties of the Mineral Oil Escaid 110.

Commercial Name	Density at 60ºF, g/cm^3	Initial Boiling Point, ºF	Final Boiling Point, ºF	Flash Point, ºF	Aniline Point, ºF	Aromatic concentration, wt%	Viscosity at 104 ºF, cSt
Escaid 110	0.806	394	459	167	162	0.05	1.63

Table 7. MOBDF A Formula.

Component	Function/Description	Quantity	Mixing time (mins)
Mineral Oil	Continuous phase	250 ml	-
Organophilic Clay (modified hectorite)	Viscosifier	6 g	5
Organophilic Clay (organo-attapulgite)	Viscosifier	6 g	5
Lime	Alkalinity Control $Ca(OH)_2$	20 g	5
Polyamide/Mineral Oil Blend	HT Primary Emulsifier	15 g	5
Glycol Ether/Fatty Acid Blend	HT Secondary Emulsifier	15 g	5
Deionized Water	Dispersed phase	25 ml	5
Calcium Chloride	Density. Clay and shale inhibition	8 g	5
Organophilic Lignite	HT Filtration Control	10 g	5
Calcium Carbonate	Weighting Material	400 g	15

Table 8. MOBDF B Formula.

Component	**Function/Description**	**Quantity**	**Mixing Time (mins)**
Mineral Oil	Continuous phase	250 ml	-
Polymer A	Primary viscosifier and filtration control agent	15 g	5
Lime	Alkalinity Control $Ca(OH)_2$	20 g	5
Polyamide/Mineral Oil Blend	HT Primary Emulsifier	15 g	5
Glycol Ether/Fatty Acid Blend	HT Secondary Emulsifier	15 g	5
Deionized Water	Dispersed phase	25 ml	5
Calcium Chloride	Density, clay and shale inhibition	8 g	5
Clay-free Sealing Agent	HT Filtration Control	5 g	5
Calcium Carbonate	Weighting Material	400 g	15

3.2 Laboratory Equipment

3.2.1 Mixer

A Hamilton mixer was used to prepare the samples. Drilling fluids were mixed by using the Multi-mixer Model 9B as shown in Figure 24. The average speeds of the impellers were 11300 rpm.

Figure 26. Hamilton Multi-mixer Model 9B.

3.2.2 Viscometer and Rheometer

A Grace M3600 Viscometer and a Grace M5600 HP/HT Rheometer were used to determine the rheological properties of the drilling fluids used in this work. Shear stress, viscosity, or gel strength were determined from the degree of rotation of the bob under the influence of the shear rate created in the mud by the action of the outer, rotating sleeve.

Figure 27. (Left) Grace M3600 Viscometer. (Right) Grace M5600 HP/HT Rheometer.

Procedure

Yield Point (YP) and Plastic Viscosity (PV) measurements:

1. Place a sample in a suitable container and immerse the rotor sleeve exactly to the inscribed line.
2. Set to the desired temperature. For example, set it to 140ºF.

3. With the sleeve rotating at 600 rpm, wait for the dial reading to reach a steady value. Record the dial reading for 600 rpm
4. Shift to 300 rpm and wait for the dial reading to come to a steady value. Record the dial reading for 300 rpm.
5. Repeat the experiment for 6 rpm and 3 rpm (optionally for 100 and 200 rpm).
6. The plastic viscosity (PV) in centipoises equals the 600 rpm reading minus the 300 rpm reading.
7. The yield point (YP) in Ibf/100 ft2 equals the 300 rpm reading minus the plastic viscosity. The temperature of the sample should be 140ºF.

Gel-Strength measurements:

1. Place the fluid sample in position as in the procedure for plastic viscosity and yield point measurement.
2. Stir at 600 rpm for a while.
3. Allow the fluid to stand undisturbed for 10 seconds. Then start stirring at 3 rpm. The maximum reading attained after starting rotation at 3 rpm is the initial gel strength.
4. Again stir the fluid sample at 600 rpm for a while and then allow the fluid to stand undisturbed for 10 minutes, then put it in 3 rpm, The measurement at the maximum reading is 10-minutes gel strength in lbf/100 ft^2.

3.2.3 Mud Balance

The density of the fluids was measured with a mud Balance shown in Figure 26. The mud balance should be calibrated frequently with fresh water. Fresh water should give a reading of 62.3 PCF at 70^{o}F.

Figure 28. Baroid Mud Balance Model 140.

Procedure

1. Put the instrument in a leveled position.

2. Fill the clean, dry cup with the fluid to be tested; make sure that some of the fluid is expelled through the hole in the cap to free trapped air.

3. Wash or wipe the fluid from the outside of the cup. Put the beam on the support and balance it by moving the rider along the graduated scale. The beam should be in the horizontal direction and the bubble in the center line. Record your reading.

3.2.4 4-Roller and 5-Roller Oven and Aging Cell

A hot rolling oven, shown in Figure 27, was used to examine the effect of heat on the rheological properties of the oil-based drilling fluids after heating at 150°F for 16 hours. Two hundred cm^3 of drilling fluid was put into the rolling oven at 150°F for 16 hours.

Figure 29. OFITE 4-Roller and 5-Roller Oven and Aging Cell.

3.2.5 Dynamic HP/HT Filter Press

The filtration mechanisms of the MOBDFs will be analyzed with the use of an OFITE Dynamic HP/HT Filter Press, Figure 28, in accordance with API standards, to simulate the filtration process under static and dynamic conditions and the effect it has on the permeability of the filter cake. This cell was selected because of its ability to simulate the downhole conditions. The dimensions of a typical Indiana Limestone core were 2.5 inches in diameter and 0.25 inch in thickness. The heterogeneity of the filter

cake was examined. The efficiency of removing the filter cake was determined by using a novel surfactant removal fluid. The tests were carried out at temperatures between 140^0F to 250° F. 250 to 500 psi differential pressures were used in all experiments to stimulate overbalance pressure in downhole condition.

Figure 30. OFITE Dynamic HP/HT Filter Press.

Procedure

1. Lubricate the O-rings. Preheat the heating jacket to a little bit above selected test temperature.
2. Load the cell with the fluid sample, take care not to fill the cell closer than ½ inch from the top.
3. Put the cell inside the equipment; make sure it is completely inside.

4. Place the cell into the heating jacket with both top and bottom valves closed. Transfer the thermometer into the thermometer well.
5. Place the pressure units on the valves and lock in place. Apply the desired differential pressure to the fluid while heating to the selected temperature.
6. Record the filtrate volume every minute. Total time of reading is 30 min
7. At the end of the test close both valves, back the T-screw off, and bleed pressure from both regulators.

3.2.6 CT-Scanner

The properties of the filter cake formed by the novel MODFs were determined and analyzed. The thickness of the filter cake build up, under different flow conditions, were measured with a CT (Computed Tomography) scanner. The relationship between the thickness of the filter cake and porosity will be developed and the permeability of the filter cake will be determined.

The objective of the X-ray computed tomography process is to obtain descriptive images of density variations within a sample. CT numbers are normalized values of the calculated X-ray absorption coefficient of a pixel (picture element) in a computed tomogram that provides radio density which is expressed in Hounsfield Units (HU). Because X-ray attenuations are related to density, the CT image gives the density distribution within every point of the object scanned. The radio density refers to a relative inability of X-rays to pass through the material and is proportional to its density (Novelline 2004; Wellington and Vinegar 1987). The average CT numbers increases

with the increase intensity. For reference, the CT number of water is 0 HU and air is -1,000 HU (Akin and Kovscek 2003).

Figure 31. CT Scanning unit at the Harold Vance Department of Petroleum Engineering.

Table 9. CT scanning settings.

X-Ray Power	150 keV
Camera Exposure	1.8 seconds
Rotation Increment	1.0°
Vertical Step	9.5 mm
Image Display Region	1024 × 1024 pixels
CT Image Resolution	1 pixel = 0.00138 mm^2
X-Ray Beam Thickness	6 pixels (0.00828 mm)

3.2.7 Core Flow Setup

Core flood experiments were performed to investigate mud solids and filtrate invasion and determine the pore blocking capabilities and retained permeability of the MOBDFs. A schematic of the core-flood unit is shown in Figure 30.

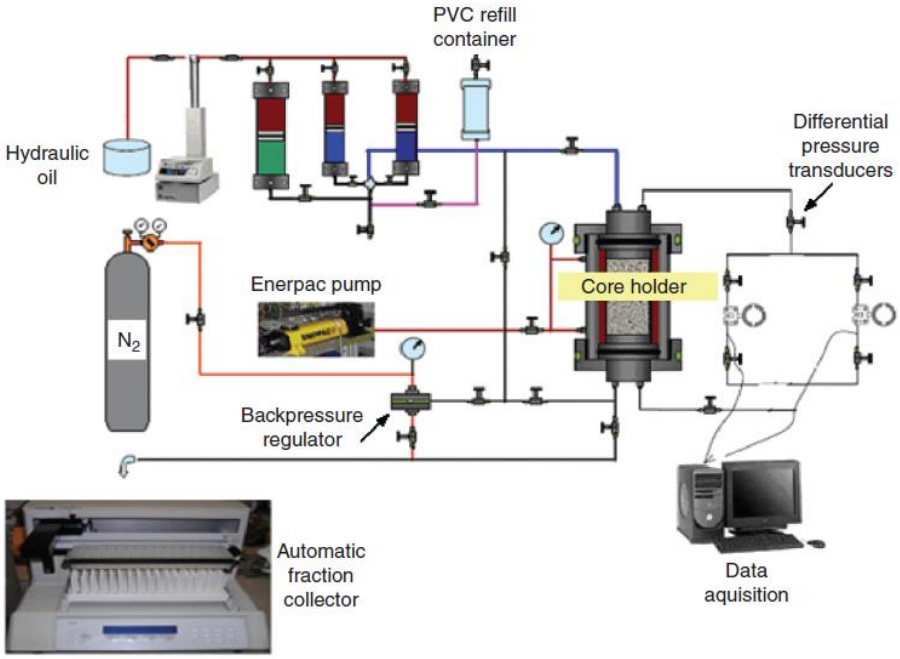

Figure 32. Core-flood set up.

3.2.8 Drop Shape Analyzer

The Drop Shape Analyzer – DSA100 is a high-quality system solution for almost all tasks in the analysis of wetting and adhesion on solid surfaces. This instrument was used for contact angle measurements.

Figure 33. Kross Drop shape analyzer (DSA 100).

3.3 Methodology / Plan of Action

1. Determine the properties of the organophilic clay additives and the polymer replacement.

1.1 Analyze the structure of the clay additives and the replacement polymer.

1.2 Evaluate additive compatibility and phase separation after hot rolling.

2. Rheological Properties of the MOBDFs at different temperatures.

2.1 Viscosity at 140, 190, and 250ºF.

2.2 PV at 140, 190, and 250ºF.

2.3 YP at 140, 190, and 250ºF.

2.4 Gel Strength at 140, 190, and 250ºF.

3. MOBDF Filtration Properties.

3.1 Spurt loss at 140ºF/300psi, 190ºF/300psi , and 250ºF/500psi

3.2 Total filtrate volume at 140ºF/300psi, 190ºF/300psi , and 250ºF/500psi

4. Filter Cake Properties

4.1 Porosity

4.2 Permeability

4.3 Filter cake removal efficiency

5. Evaluation of Formation Damage.

5.1 Determine retained permeability of each core after filter cake removal

6. Evaluation of Formation Wettability

6.1 Measure contact angle of between MOBDFs and the rock

6.2 Determine emulsion breakdown efficiency

4. RESULTS OF EXPERIMENTS

4.1 Chemical Composition of Additives Used in MOBDF A and B

4.1.1 Viscosifier in MOBDF A

Organophilic clay (modified hectorite)

Wet processed organophilic clay used as gallant/suspension agent in the HP/HT oil-based mud system. Is temperature stable up to 425°F (218°C).

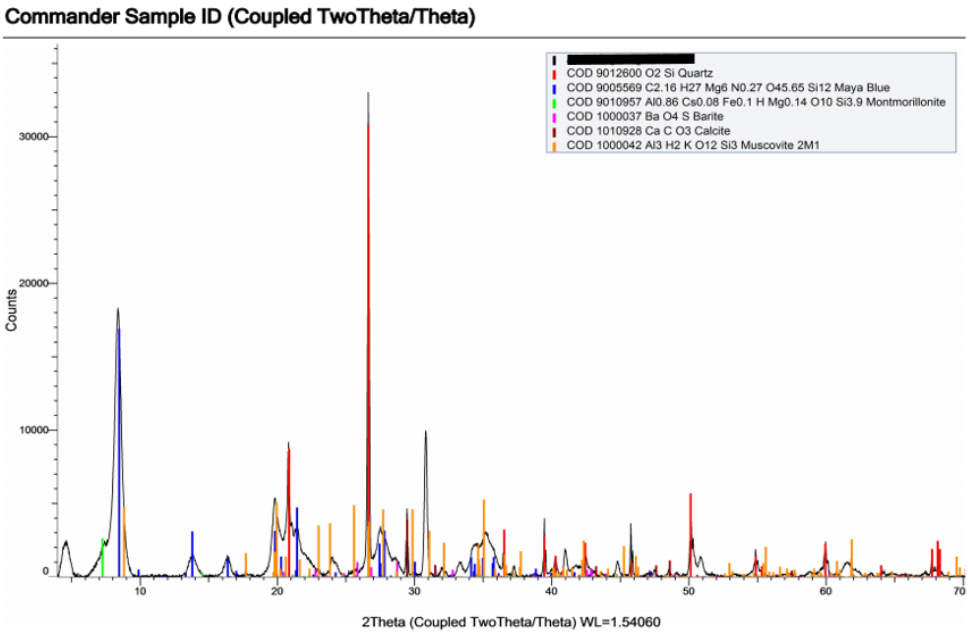

Figure 34. X-ray diffraction spectrum of organophilic clay viscosifier sample.

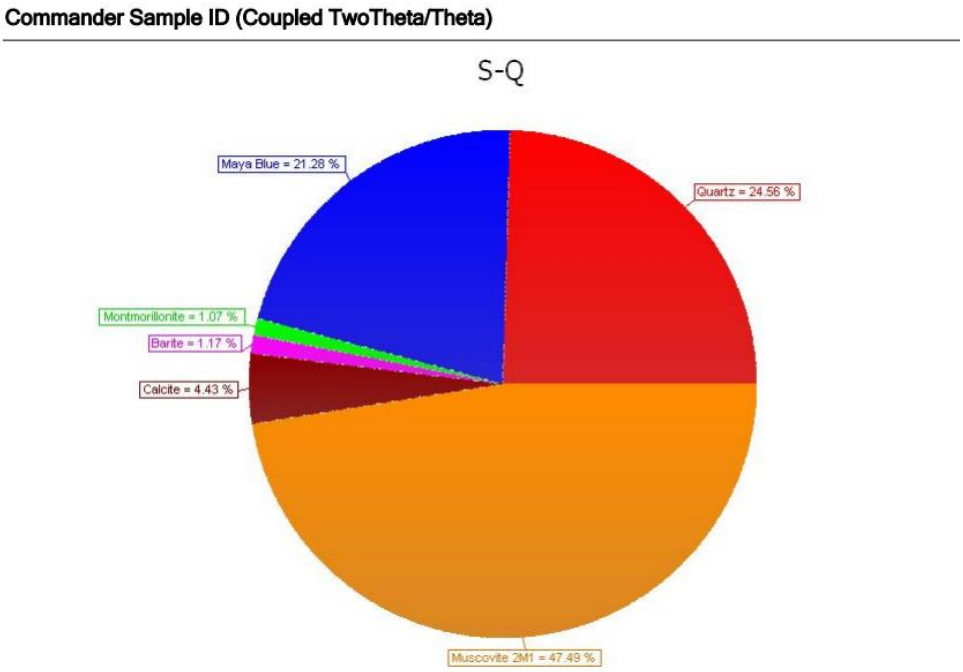

Figure 35. Composition of organophilic clay viscosifier sample.

4.1.2 HT Filtration Control Additive in MOBDF A

Organophilic Lignite

An organophilic lignite additive used in emulsion-based drilling fluid systems to improve filtration control at high temperatures. Lignite is used as a filtration control agent and as a secondary deflocculant. To solubilize lignite, it must have a highly alkaline environment. It functions as a fluid loss additive up to 400°F. Compared to lignosulfonate, lignite provides better filtration control at elevated temperatures. It is usually added with lignosulfonate.

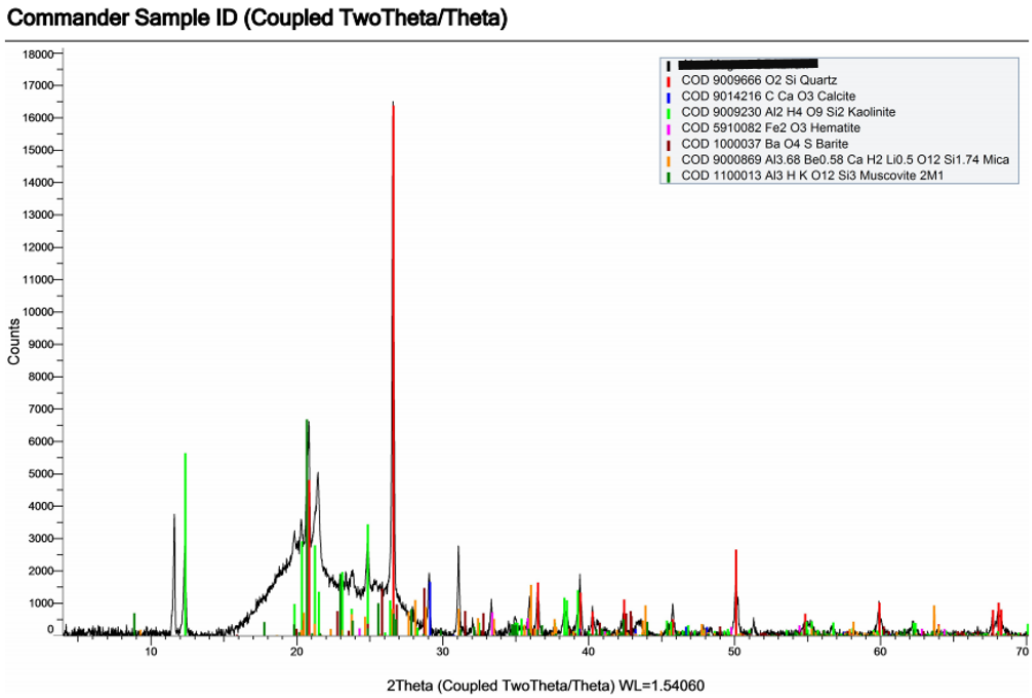

Figure 36. X-ray diffraction spectrum of the organophilic lignite sample.

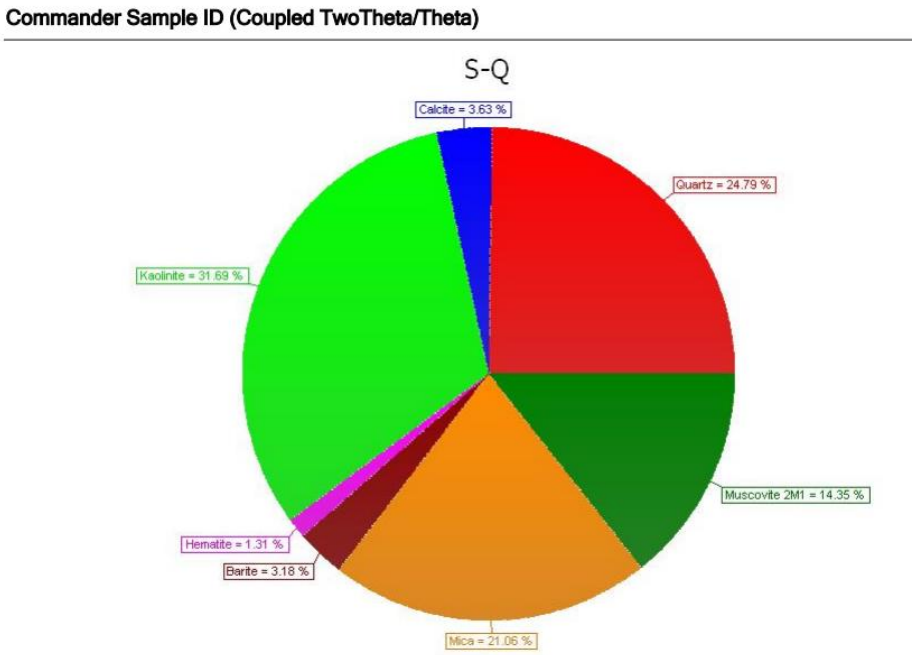

Figure 37. Composition of the of the organophilic lignite sample.

4.1.3 Polymer Additive in MOBDF B

Polymer A

The filtration control agent is a cross-linked polymer that can provide filtration control in all non-aqueous systems up to about 425°F (218°C). It can also provide secondary viscosity and is suitable for use in fluids designed for deep water applications. Polymer A was the primary filtration control agent for the clay-free invert emulsion fluid used in this work.

Applications/Functions

1. Can reduce HP/HT in all oil and synthetic mud systems in temperature ranges up to 425°F (218°C).
2. Can provide secondary viscosity.

Properties

1. Appearance: Off-white powder.
2. Specific gravity: 1.03

Figure 38. Polymer A

4.2 Rheological Properties of MOBDF A and B

The main objective of this project was to develop an organophilic clay-free drilling fluid formula capable of performing similarly to an already tested drilling fluid formula containing organophilic clay additives. Polymer A was used as a viscosifier and filtration control agent in MOBDF B as previously stated. The performance and stability of MOBDF B was examined and compared to the performance of MODF A. The density of both drilling fluids was kept constant for all the experiments and measured at room temperature. The properties of MOBDF A and B are given in Table 10 and Table 11 after aging them for 16 hours at 150^{o}F. The rheology was resolved with the Bingham Plastic and Power Law models. Properties where measured at 120^{o}F.

MOBDF A

Table 10. MOBDF A properties after aging at 150°F for 16 hrs.

Properties	MOBDF A
Density, lb/ft^3	101
Plastic Viscosity, cp	15
Yield Point, lb/100 ft^2	16
10 s gel strength, lb/100 ft^2	8
10 min gel strength, lb/100 ft^2	58

MOBDF B

Table 11. MOBDF B properties after aging at 150°F for 16 hrs.

Properties	MOBDF B
Density, lb/ft^3	100
Plastic Viscosity, cp	10
Yield Point, lb/100 ft^2	14
10 s gel strength, lb/100 ft^2	6
10 min gel strength, lb/100 ft^2	38

MOBDF A and B Comparison at Temperatures and Shear Rates

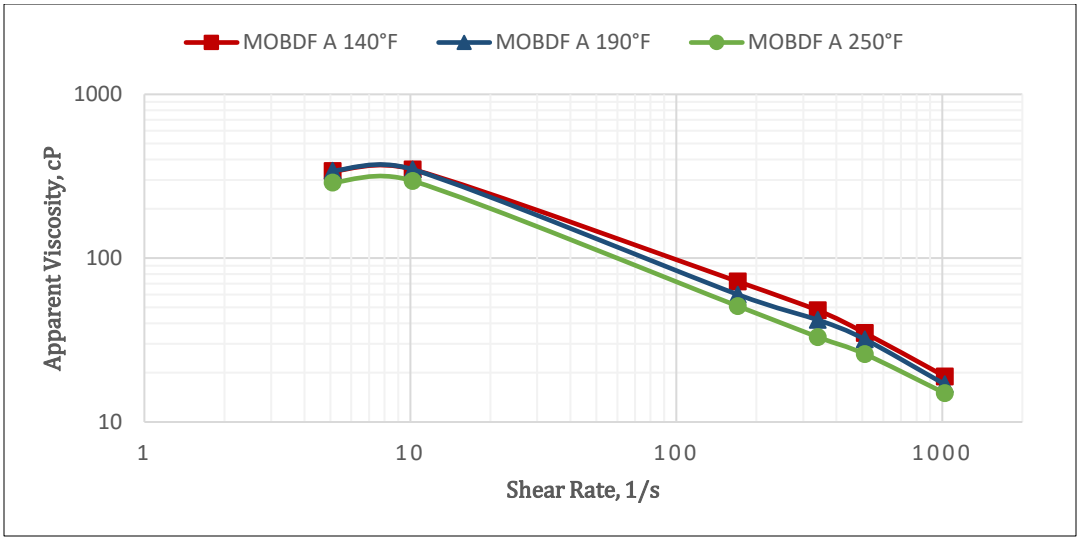

Figure 39. Apparent viscosity behavior of MOBDF A at different shear rates and temperatures.

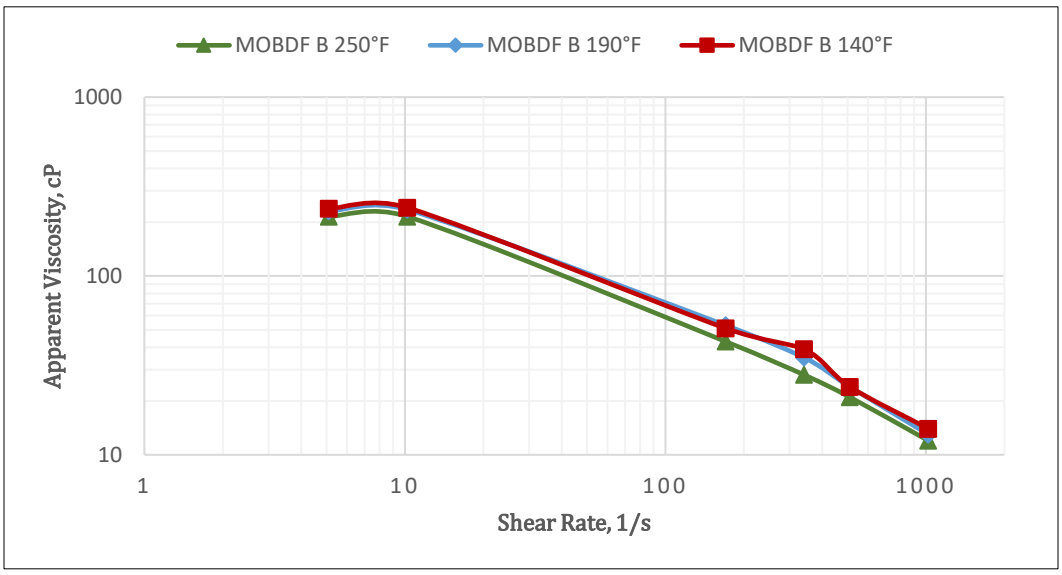

Figure 40. Apparent viscosity behavior of MOBDF B at different shear rates and temperatures.

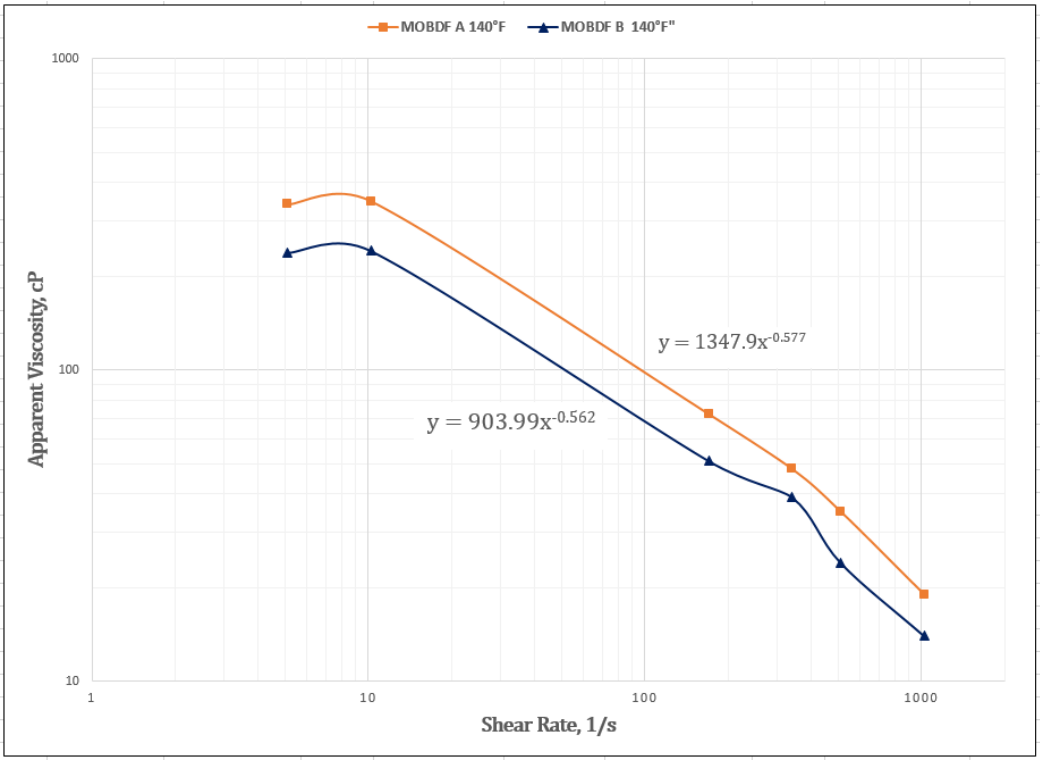

Figure 41. Apparent viscosity comparison between MOBDF A and B at 140°F.

Table 12. Comparison between MOBDF A and B properties at 140°F.

Properties	MOBDF A	MOBDF B
Density, lb/ft^3	101	99
Plastic Viscosity, cp	16	10
Yield Point, lb/100 ft^2	16	14
10 s gel strength, lb/100 ft^2	8	6
10 min gel strength, lb/100 ft^2	62	38

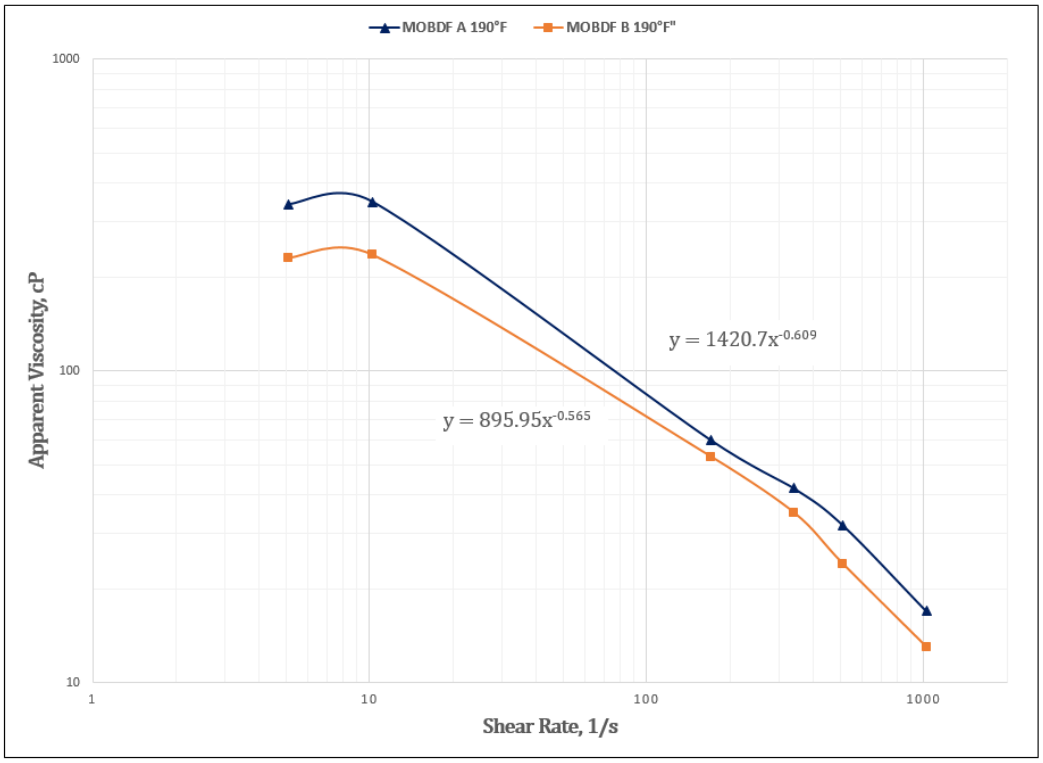

Figure 42. Apparent viscosity comparison between MOBDF A and B at 190°F.

Table 13. Comparison between MOBDF A and B properties at 190°F.

Properties	MOBDF A	MOBDF B
Density, lb/ft^3	100	100
Plastic Viscosity, cp	15	11
Yield Point, lb/100 ft^2	17	13
10 s gel strength, lb/100 ft^2	9	6
10 min gel strength, lb/100 ft^2	62	36

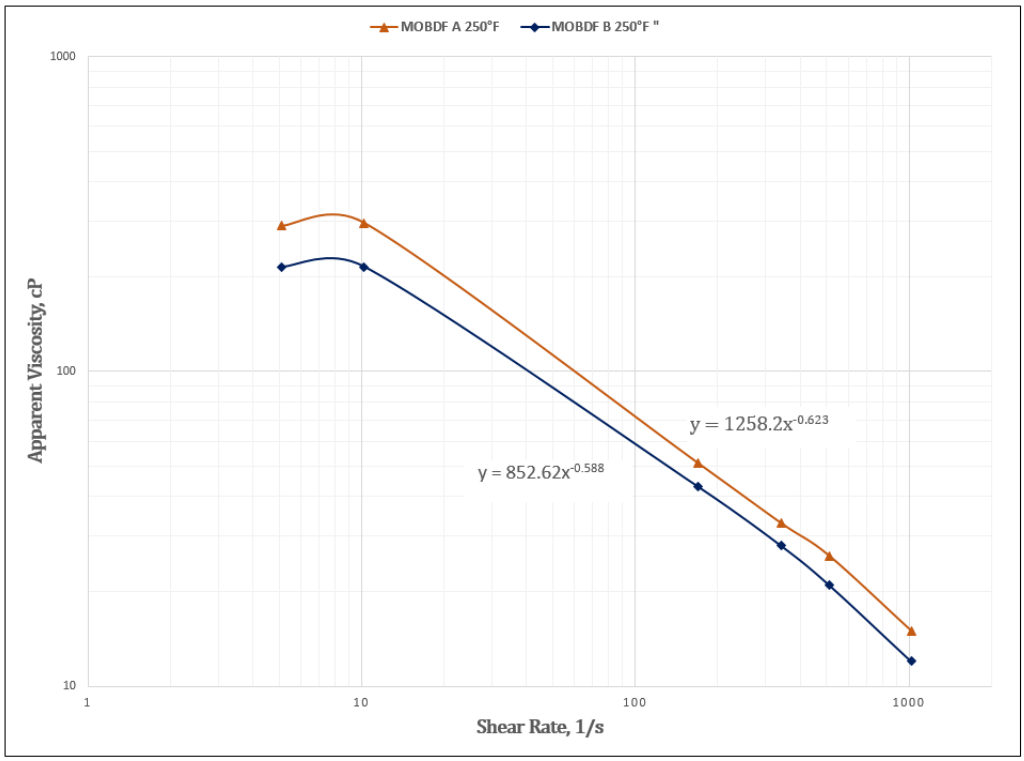

Figure 43. Apparent viscosity comparison between MOBDF A and B at 250°F.

Table 14. Comparison between MOBDF A and B properties at 250°F.

Properties	MOBDF A	MOBDF B
Density, lb/ft^3	101	100
Plastic Viscosity, cp	11	9
Yield Point, lb/100 ft^2	15	12
10 s gel strength, lb/100 ft^2	8	6
10 min gel strength, lb/100 ft^2	65	35

4.3 Filtration Control of MOBDF A and B

Filtration tests were conducted using the HP/HT filter press under static conditions. Both drilling fluids were put in the cell and the temperature and pressure

were adjusted to 140°F/300 psi, 190°F/300 psi, and 250°F/500 psi. High permeability Indiana limestone cores with a thickness of 1 in. and a diameter of 2.5 in. were used for this experiment. First, the filter cake was formed at this temperature and pressure. The filtrate was collected over a 30-minute interval and the results of the fluid loss experiments are given in Figures 44 and 45 respectively. It shows that the fluid loss was more prominent for MOBDF A.

Relation of filtrate volume to the square root of time

HP/HT filtration results for constant differential pressure are usually plotted as cumulative filtrate volume versus square root of time. This is because theoretically, cumulative filtrate volume is proportional to the square root of time for constant differential pressure. In general, the line of cumulative filtrate volume does not pass through the origin, as indicated in Figure 44 due to the spurt loss to the formation before a filter cake is formed. The spurt loss and the cumulative filtrate volume of every experiments were recorded in Tables 15 and 16.

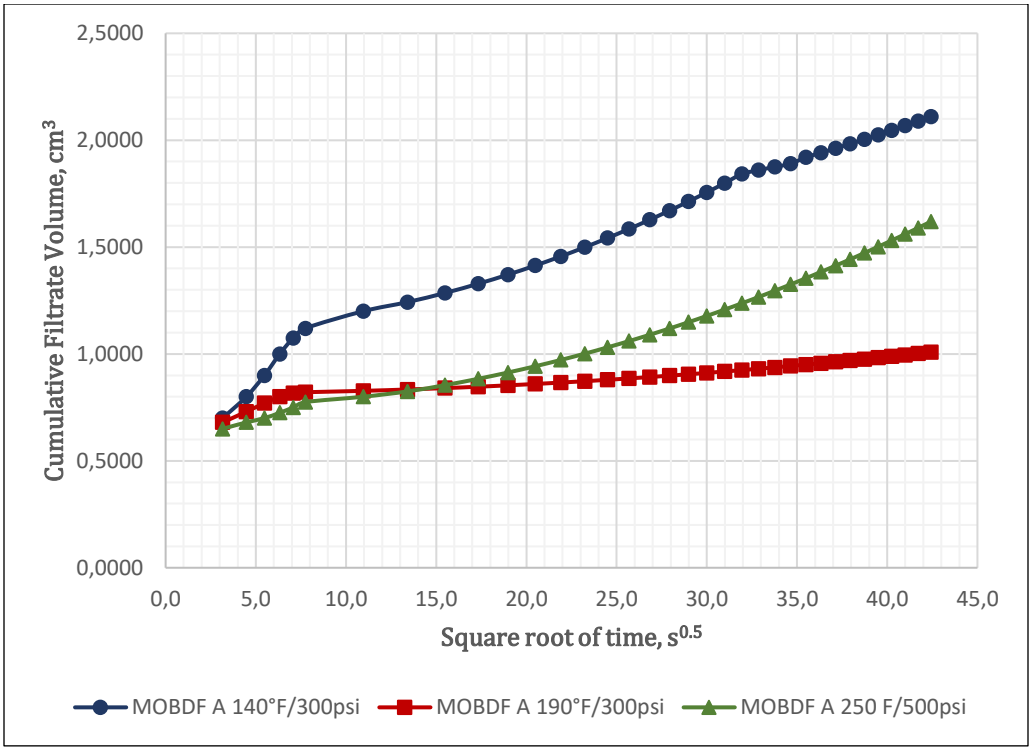

Figure 44. Cumulative filtrate volume as a function of the square root of the time under static conditions for MOBDF A at 140, 190, and 250°F.

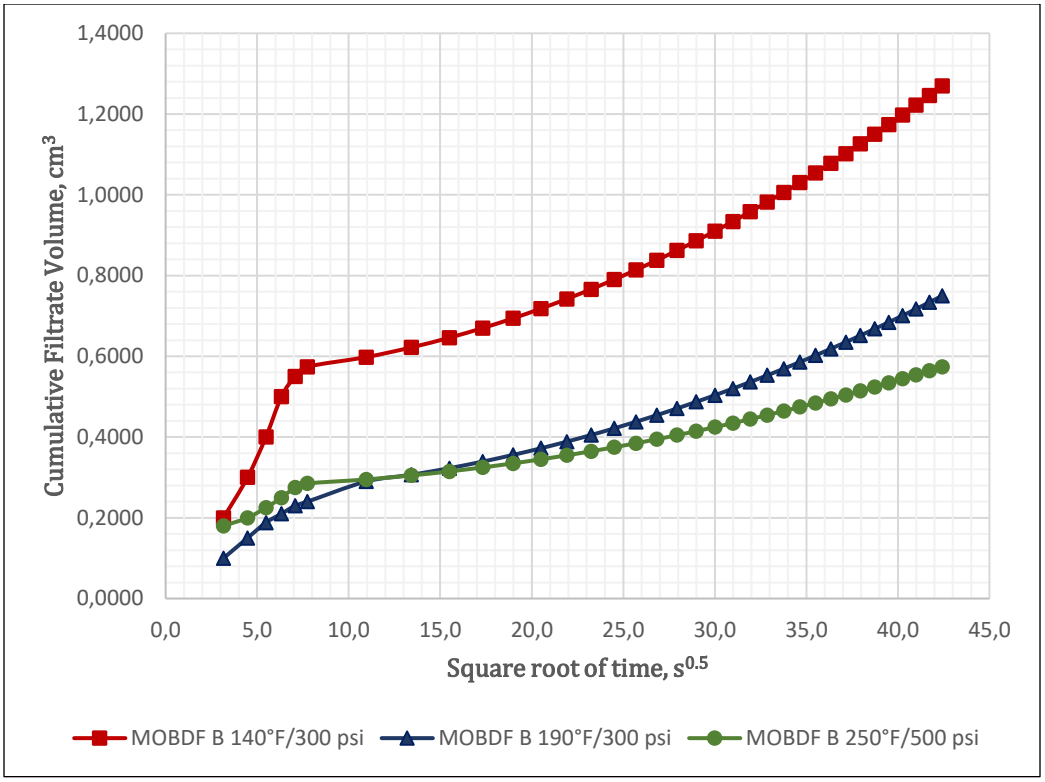

Figure 45. Cumulative filtrate volume as a function of the square root of the time under static conditions for MOBDF B at 140, 190, and 250°F

Table 15. Spurt Loss MOBDFs.

Experimental Conditions	**Spurt Loss MOBDF A, ml**	**Spurt Loss MOBDF B, ml**
140°F/300 psi	0.4	0.1
190°F/300 psi	0.6	0.05
250°F/500 psi	0.6	0.1

Table 16. Cumulative Filtrate Volume MOBDFs.

Experimental Conditions	Filtrate Volume MOBDF A, ml	Filtrate Volume MOBDF B, ml
140°F/300 psi	2.2	1.3
190°F/300 psi	1.0	0.8
250°F/500 psi	1.6	0.6

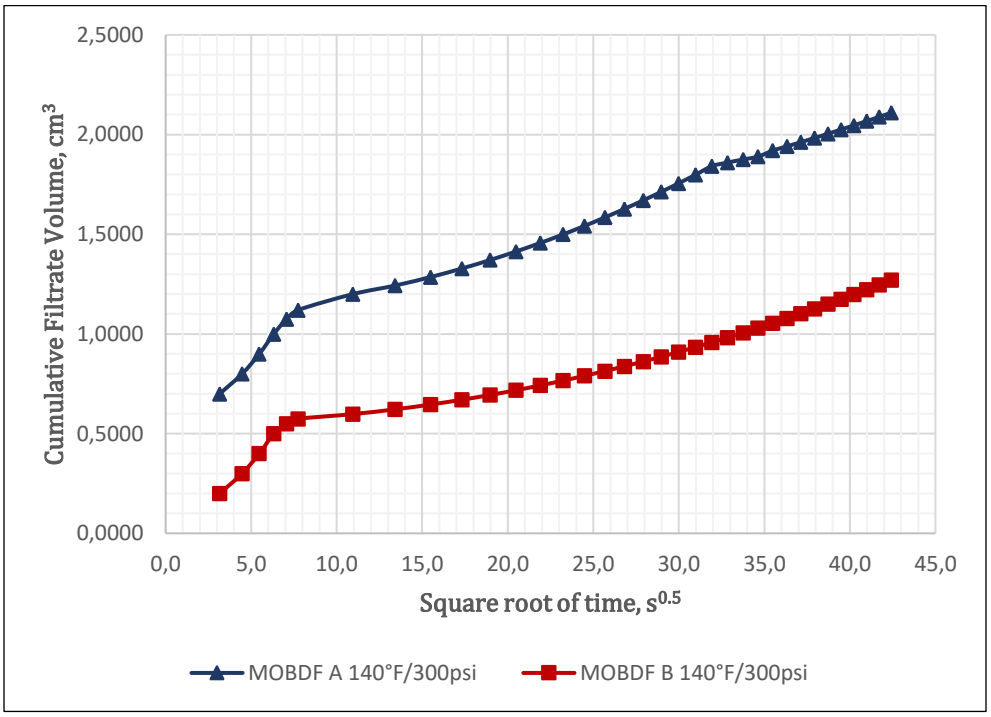

Figure 46. Cumulative filtrate volume as a function of the square root of the time under static conditions. Comparison between MOBDF A and B at 140°F.

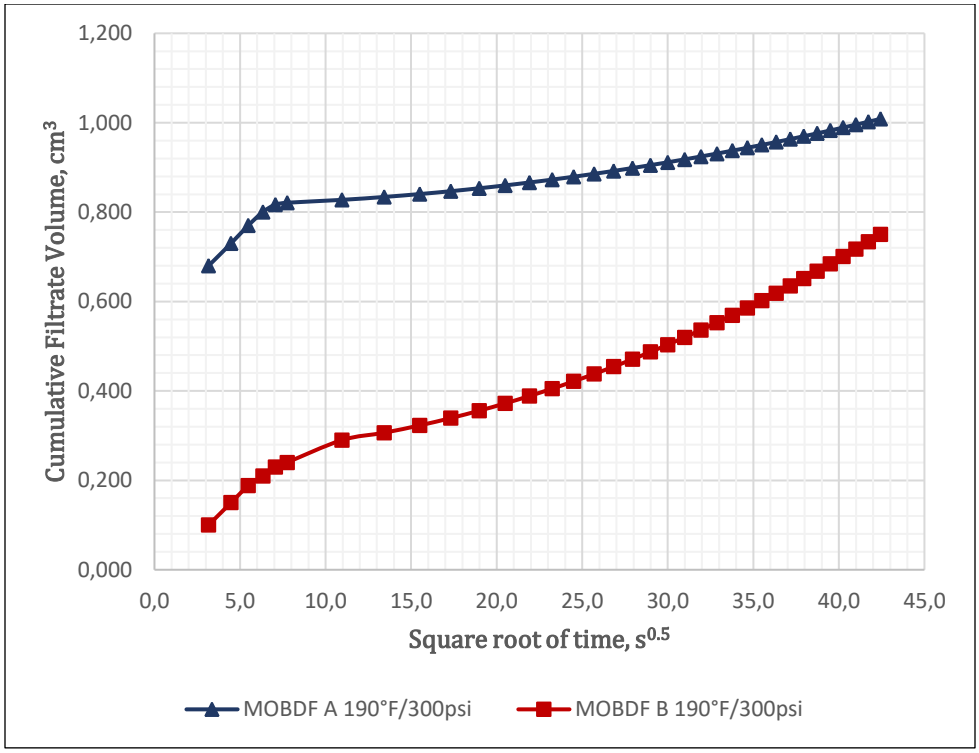

Figure 47. Cumulative filtrate volume as a function of the square root of the time under static conditions. Comparison between MOBDF A and B at 190°F.

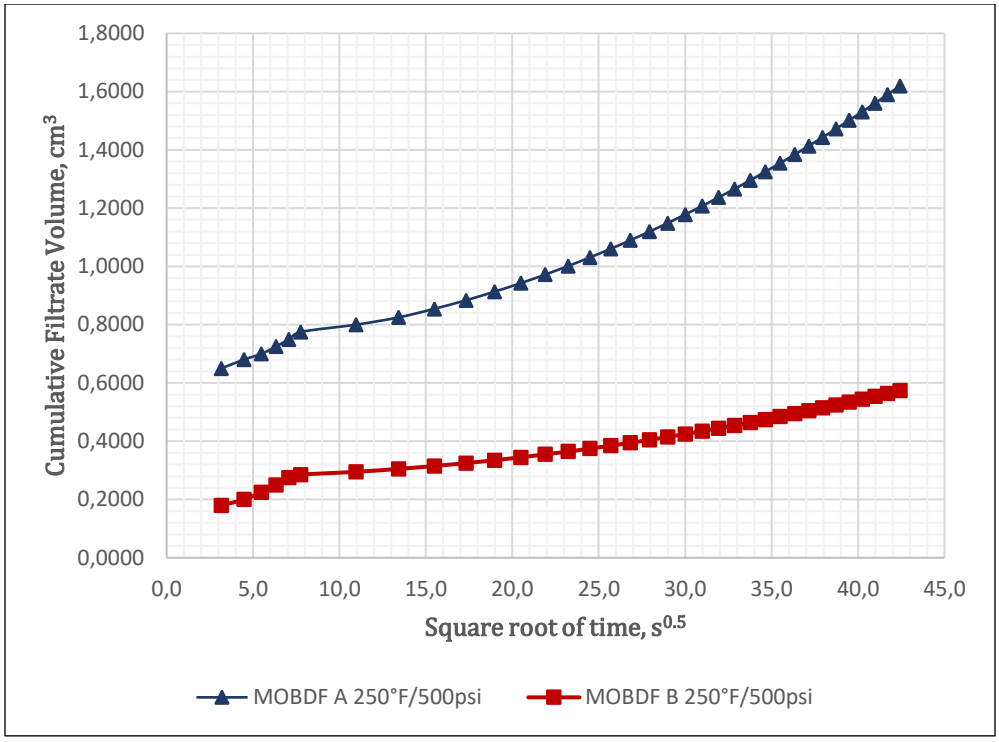

Figure 48. Cumulative filtrate volume as a function of the square root of the time under static conditions. Comparison between MOBDF A and B at 250°F.

4.4 Filter Cake Thickness

The thickness of the deposited filter cakes varies considerably depending on the composition of the muds, depositional environments, nature of interactive forces prevailing during the period of deposition, etc. Which is why the formed filter cake can provide valuable information about the drilling fluid quality and can help take corrective measures in designing a drilling fluid. Formation of a thick filter cake during static filtration indicates the possibility of formation of a thick cake on the borehole wall during the period of non-circulation with a reduction in hole diameter. This will cause an

increase in the angle of contact between the cake and drill collar in case of a pipe stuck problem. Figures 49 through 54 show the thicknesses of the filter cakes formed during static filtration under the conditions already specified. The thicknesses of the filter cakes formed by MOBDF B were slightly lower than MOBDF A in some cases.

Figure 49. Filter cake thickness formed by MOBDF A at 140^{o}F/300 psi.

Figure 50. Filter cake thickness formed by MOBDF A at 190^{o}F/300 psi.

Figure 51. Filter cake thickness formed by MOBDF A at 250°F/500 psi.

Figure 52. Filter cake thickness formed by MOBDF B at 140°F/300 psi.

Figure 53. Filter cake thickness formed by MOBDF B at 190°F/300 psi.

Figure 54. Filter cake thickness formed by MOBDF B at 250^{o}F/500 psi.

4.5 Filter Cake Porosity

The formation of a filter cake and the invasion of filtrate in the formation change the near wellbore reservoir characteristics in course of time. These changes affect the readings of logging tools such as resistivity log, density log and neutron log. Cake properties have numerous applications both in drilling and reservoir engineering analyses. These properties also play a key role in numerical modelling of mud-related drilling and reservoir engineering problems. Filter cake properties such as permeability and porosity are important parameters for permeability determination in low permeable formations during drilling.

4.6 Porosity Determination

The Indiana limestone cores were scanned before each experiment in dry and wet conditions to determine their initial porosity.

1. Dry conditions: Each core was dried in the oven for 16 hrs at 150^{o}F.
2. Wet conditions: Each core was saturated with a 5wt% KCl brine for 48 hours prior to the day of the experiment.

The porosity of each core was determined using equation 13 and the results recorded in Table 17.

$$\phi = \frac{CT_{wet} - CT_{dry}}{CT_{brine} - CT_{air}} \qquad \text{.....(13)}$$

where,

CT_{wet} = CT number of the core after being saturated with the KCl brine

CT_{dry}= CT number of the dry core

CT_{brine} = CT number of the KCl brine, (CTN = 53.89)

CT_{air} = CT number of air, (CTN = -1000)

Table 17. Initial porosity of Indiana Limestone cores

Core #	Porosity, ϕ
1	25%
2	27%
3	30%
4	23%
5	25%
6	28%

The porosity of the filter cake formed by the MOBDFs was determined similarly using equation 13. The results are shown in Table 18 below:

Table 18. Porosity of the filter cakes formed by the MOBDFs.

Core #	Experimental Conditions	Porosity, ϕ
1	MOBDF A 140°F/300 psi	8%
2	MOBDF A 190°F/300 psi	5%
3	MOBDF A 250°F/500 psi	7%
4	MOBDF B 140°F/300 psi	2.5%
5	MOBDF B 190°F/300 psi	2.5%
6	MOBDF B 250°F/500 psi	3.5%

4.7 Filter Cake Removal Efficiency

The efficiency of removing the filter cake was done by measuring the weight of the Indiana limestone core after being saturated in the 5wt% KCl brine for 48 hours. After forming the filter cake at the desired temperature and pressure with the MOBDFs, the weight of the core was measured a second time. A third and final weight measurement was taken after soaking the core in the removal solution for 6 hours. Efficiency was calculated using equation 14 based on weight differences before and after the filter cake removal treatment.

$$Efficiency = \frac{w_2 - w_3}{w_2 - w_1} \quad \text{..... (14)}$$

where,

w_1 = weight of the Indiana limestone core saturated in 5wt% KCl brine

w_2 = weight of the Indiana limestone core with formed filter cake

w_3 = weight of the Indiana limestone core after removal treatment

Tables 19 and 20 give the efficiency of filter cake removal for MOBDF A and B, respectively, at the different experimental conditions.

Table 19. Efficiency of filter cake removal for MOBDF A

	Experimental Conditions		
Measured weights, g	140°F /300 psi	190°F /300 psi	250°F /500 psi
w_1	49.8	45.3	48.2
w_2	57.8	54.6	56.8
w_3	50.4	46.5	48.8
Efficiency (%)	91.3	90.5	93.1

Table 20. Efficiency of filter cake removal for MOBDF B

	Experimental Conditions		
Measured weights, g	140°F /300 psi	190°F /300 psi	250°F /500 psi
w_1	49.3	48.9	49.6
w_2	56.6	55.4	57.4
w_3	49.9	49.3	50.3
Efficiency (%)	91.6	92.4	91.8

4.8 Filter Cake Permeability

Depending on the porosity of the filter cake obtained from the CT scan, Khatib (1994) provided an empirical relationship to obtain the permeability of the filter cake shown in equation 15.

$$k_c = 112.7 * e^{-8.8(1-\phi_c)} \quad \text{..... (15)}$$

k_c = permeability of the filter cake

ϕ_c = porosity of the filter cake

The results of the calculated permeabilities of the filter cakes formed by MOBDFs A and B are shown in Table 21.

Table 21. Filter cake permeability using MOBDF A and B.

	Experimental Conditions		
Permeability (k_c), md	140°F /300 psi	190°F /300 psi	250°F /500 psi
MOBDF A	0.034	0.026	0.031
MOBDF B	0.021	0.021	0.023

4.9 Evaluation of Formation Damage

4.9.1 Retained Permeability

Coreflood tests were performed to determine the removal efficiency of the filter cakes generated by MOBDF A and B at a temperature of 250°F. The back pressure and overburden pressures were set at 1100 psi and 1600 psi, respectively. Indiana limestones cores were used for the test.

The initial permeability of each core used in these experiments was measured using Darcy's law, Equation 16.

$$k = \frac{122.812 * q * \mu * h}{\Delta p * d^2} \qquad \text{.....(16)}$$

where,

k = permeability of the core, md

q = flow rate, cm^3/min

μ = fluid viscosity, cp

h = core thickness

Δp = differential pressure, psi

d = diameter through which the brine solution will flow, in

The time required to flow 1 pore volume (PV) of 5 wt% KCl brine at a constant pressure was recorded. The same procedure was performed after the removal of the filter cake to calculate the final permeability. The retained permeability was calculated using equation 17.

$$k_r = \frac{k_f}{k_i} * 100\% \quad \text{..... (17)}$$

where,

kr = retained permeability, md

kf = final permeability, md

ki = initial permeability, md

The core pore volume (PV) was calculated from the density of the brine (ρ_{brine} = 1.03 g/cm^3 at 70^{o}F) and the weight difference in both dry and saturated cases of the Indian limestone cores as shown in Equation 18.

$$PV = \frac{w_{sat} - w_{dry}}{\rho_{brine}} \quad \text{.....(18)}$$

where,

PV = pore volume of the Indian limestone core

w_{sat} = weight of the Indiana limestone core saturated in 5wt% KCl brine

w_{dry} = weight of the Indiana limestone core after being dried

ρ_{brine} = density of the 5 wt% KCl brine

The results of the retained permeabilities after removing the filter cakes generated by MOBDFs A and B are shown in Table 22.

Table 22. Retained Permeabilities

Core ID	MOBDF Used	Pore Volume, cm^3	Initial Permeability, md	Final Permeability, md	Retained Permeability, %
IndiA	A	9.26	100.75	78.14	77.56
IndiB	B	9.67	100.34	89.33	89.04

4.9.2 Rock Wettability

Drop Shape Analysis (DSA) was used to determine the wettability of MOBDF A and B and the effectiveness of the filter cake removal treatment to breakdown the drilling fluids at 250^{o}F/500 psi. Five sandstone disks were dried for 12 hours at 140^{o}F and labeled disk 1, 2, 3, 4, 5, 6, respectively. Table 23 shows the minerology of the Berea sandstone disks used for DSA.

Disk 1, was saturated with a 5wt% brine KCl for 24 hours to measure the initial wettability of sandstone disk. Disks 2 and 3, were saturated in MOBDF A and B emulsion, respectively, for 24 hours to measure the wettability of sandstone disk after being in contact with the MOBDFs emulsion. Finally, Disks 4 and 5 were saturated with a blend of MOBDF A and B emulsion, respectively, and the removal treatment (1:1 ratio) for 24 hours, to measure the effectiveness of the removal treatment to break down the MOBDFS.

The contact angle was measured using the captive drop method, with the injection of a crude oil droplet on to the sandstone disk's surface. The crude oil drop was maintained on the disk's surface for at least 2 minutes before using Drop Shape Analysis software to capture the drop image and the contact angle value. The resulting measurements were recorded in Table 24 and 25.

Table 23. Minerology of Berea sandstone cores

Minerology	Quartz	Kaolinite	Microline	Muscovite	Smectite
Concentration, wt%	91	3	4	1	1

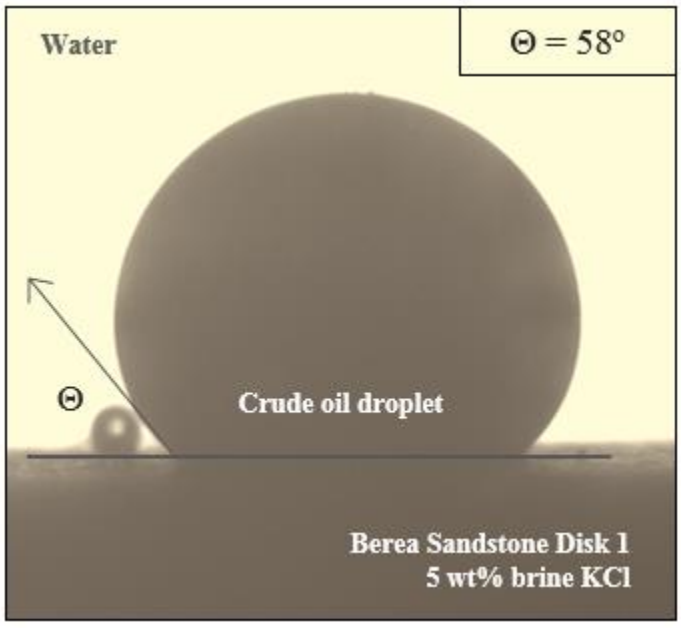

Figure 55. Contact angle measurement of disk 1 at 250°F/500 psi.

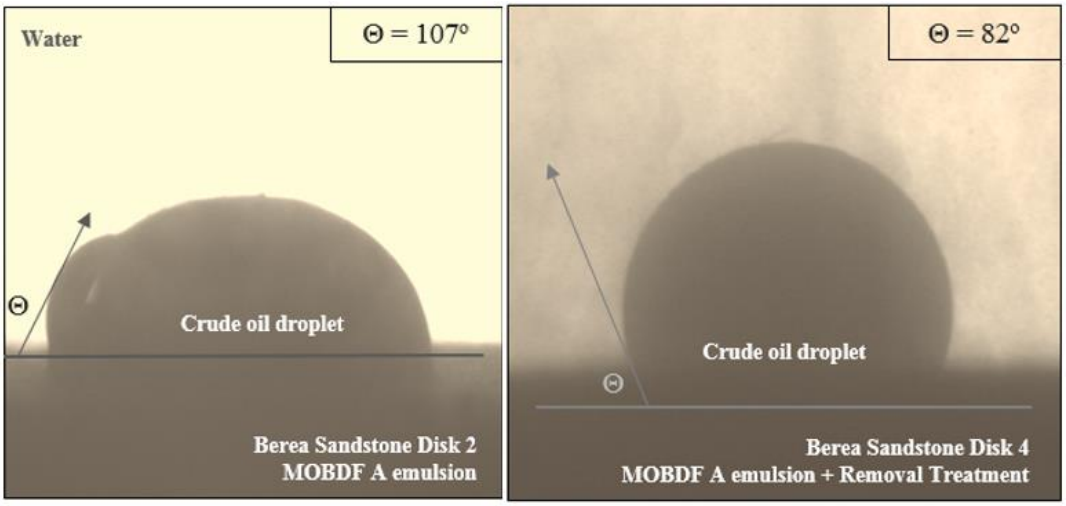

Figure 56. Contact angle measurements of disk 2 and 4. Using MOBDF A at 250°F/500 psi.

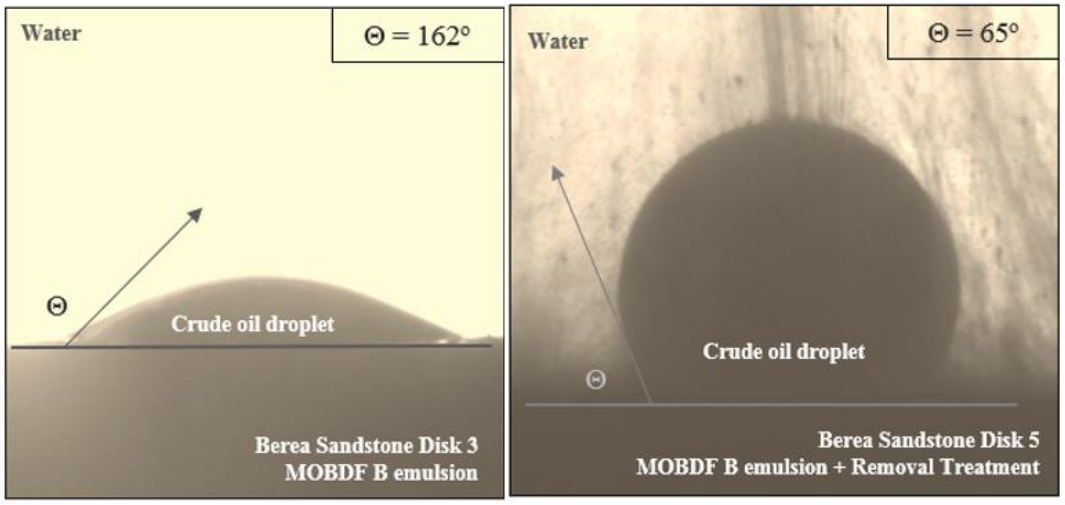

Figure 57. Contact angle measurements of disk 3 and 5. Using MOBDF B at 250°F/500 psi.

Table 24. DSA contact angle measurements.

Disk ID	Saturated in with	Contact Angle, ^{o}	Wettability
Disk 1	5wt% brine KCl	58	Water-wet
Disk 2	MOBDF A	107	Oil-wet
Disk 3	MOBDF B	162	Oil-wet
Disk 4	MOBDF A + Removal treatment	82	Oil-wet
Disk 5	MOBDF B + Removal treatment	65	Oil-wet

$$MOBDF\ Breakdown\ Efficiency = \frac{\theta_{MOBDF} - \theta_{MOBDF+\ removal\ treat}}{\theta_{\ MOBDF}} \quad \ldots\ldots\ldots\ldots (19)$$

where,

$\Theta_{\ MODF}$ = Measured contact angle with disk saturated by MOBDF

$\Theta_{\ MOBDF\ +\ Removal\ treat}$ = Measured contact angle with disk saturated by MOBDF + Removal treatment

Table 25. MOBDFs breakdown efficiency.

Breakdown Efficiency, %	
MOBDF A	23.11
MOBDF B	59.86

5. CONCLUSIONS

The experiments carried out in this work revealed that a clay-free mineral oil-based drilling fluid formula can be developed successfully by replacing all organophilic clay additives with a cross-linked polymer as a viscosifier and filtration control agent. Based on the results obtained from the rheology tests performed on the clay-free mineral oil-based drilling fluid, we can conclude that the viscosity and suspension characteristics of this drilling fluid were slightly improved compared to a drilling fluid containing organophilic clay additives. The apparent viscosity of MOBDF B was lower (PV= 9-11 cp) than the apparent viscosity of MOBDF A (PV= 11-16 cp) when subjected to different temperatures. MOBDF B also exhibited good ability to suspend cuttings (YP= 14 lb/100 ft^2) at different temperatures and pressures. The clay-free mineral oil-based drilling fluid exhibited good filtration properties a thin filter cake ($\leq$ 0.06 in), small filtrate volume ($\leq$1.3 ml), small spurt loss ($\leq$0.1 ml), and a filter cake permeability less than 0.04 md under the experimental conditions set for this stud. The removal efficiency of the filter cake generated by the clay-free mineral oil-based drilling fluid was very similar to the removal efficiency of the drilling fluid containing organophilic clay additives (90-93%). After filter cake removal, the retained permeability measured for the clay-free mineral oil-based drilling fluid (89.04%) was higher than the retained permeability attained after removing the filter cake formed by the drilling fluid containing organophilic clay additives (77.56%).

6. FUTURE WORK

After considering the positive performance under the experimental parameters set for the clay-free mineral oil-based drilling fluid formula, it would be ideal to assess its performance under more severe conditions. Test the ability of the drilling fluid formula to build viscosity and gel strength in high pressure and high temperature (HP/HT) wellbore conditions and low temperatures (inside risers). Evaluate and characterize the filter cake formed by the clay-free mineral oil-based drilling fluid formula using different weighting materials, and determine the most efficient way to remove it.

The suggested experimental plan is described below:

1. Determine the rheological properties of the clay-free mineral oil-based drilling fluid formula at the following range of temperatures:
   1.1 Viscosity at 5, 10, 400, and 450ºF
   1.2 PV at 5, 10, 400, and 450ºF
   1.3 YP at 5, 10, 400, and 450ºF
   1.4 Gel Strength at 5, 10, 400, and 450ºF

2. Determine the rheological properties of the clay-free mineral oil-based drilling fluid formula at the following range of wellbore conditions:
   2.1 5°F/1000psi, 5°F/2000psi, 5°F/3000psi, 5°F/4000psi
   2.2 10°F/1000psi, 10°F/2000psi, 10°F/3000psi, 10°F/4000psi
   2.3 400°F/1000psi, 400°F/2000psi, 400°F/3000psi, 400°F/4000psi

2.4 450°F/1000psi, 450°F/2000psi, 450°F/3000psi, 450°F/4000psi

3. Test different weighting materials for the clay free mineral oil-based drilling fluid formula:

3.1 Ilmenite ($FeTiO_3$)

3.2 Manganese Tetroxide (Mn_3O_4)

5. Test the efficiency of different removal treatments to remove the filter cake generated by the clay free mineral oil-based drilling fluid formula.

5.1 Acids

5.2 Chelating agents

5.3 Oxidizers

5.4 Enzymes

REFERENCES

Ackal, K., and Gillikin, A. 2010. Clay-Free Synthetic-Based Fluid Provides High-Angle Wellbore Stability with Minimal Dilution and Treatment Requirements, paper SPE 127560 presented at the 2010 IADC/SPE Drilling Conference and Exhibition, New Orleans, Louisiana, USA, 2-4 February 2010.

Akin, S. and Kovscek, A.R. 2003. Computed Tomography in Petroleum Engineering Research. Geological Society, London, Special Publications 215 (1): 23-38.

Al Moajil, A.M., and Nasr-El-Din, H. 2011. Formation Damage Caused by Improper Mn_3O_4-Based Filter Cake Cleanup Treatments, paper SPE 144179 presented at the European Formation Damage Conference, Noordwyk, The Netherlands, 5-7 June.

Alotaibi, M.B., Nasr-El-Din, H.A., Hill, A.D., Al Moajil, A.M. 2007. An Optimized Method to Remove Filter Cake Formed by Formate Based Drill-in Fluid in Extended Reach Wells. Paper SPE 109754 presented at Asia Pacific Oil and Gas Conference and Exhibition, Jakarta, Indonesia. 30 October-1 November.

Al-Yami, A.S., Nasr-El-Din, H.A., Bataweel, M.A. et al. 2008. Formation Damage Induced by Various Water-based Fluids Used to Drill HP/HT Wells. Paper SPE 112421-MS presented at the SPE International Symposium and Exhibition on Formation Damage Control, Lafayette, Louisiana, USA, 13-15 February.

Amani, M., M Al-Jubouri, A. Shadravan. 2012. Comparative Study of Using Oil-Based Mud Versus Water-Based Mud in HP/HT Fields. Advances in Petroleum Exploration and Development. Vol. 4. Iss. 2. Pag. 18-27.

Bageri, B.S., Al-Mutairi, S.H., and Mahmoud, M.A. 2013. Different Techniques for Characterizing the Filter Cake, paper SPE 163960 presented at the SPE Middle East Unconventional Gas Conference and Exhibition, Muscat, Oman, 28-30 January.

Baker Hughes. 2006. Chapter 1- Fundamentals of Drilling Fluids. In Drilling Fluids Reference Manual, 1-133.

Baker Hughes. 2006. Chapter 5- Oil/Synthetic Drilling Fluids. In Drilling Fluids Reference Manual, 211-280.

Bourgoyne, A. T., Jr., K. K. Millheim, M. E. Chenevert et al. 1986. Applied Drilling Engineering, Society of Petroleum Engineers (Reprint). SPE-31656-MS

Bourgoyne, A.T., Millheim, K.K., Chenevert, M.E., and Young, F.S. 1991. Applied Drilling Engineering (revised printing), Textbook Series, SPE, Richardson, Texas 2.

Burrows, K., Carbajal, D., Kirsner, J. et al. 2004. Benchmark Performance: Zero Barite Sag and Significantly Reduced Downhole Losses with the Industry's First Clay-Free Synthetic-Based Fluid paper SPE 87138 presented at the IADC/SPE Drilling Conference, Dallas, Texas, USA, 2-4 March.

Carbajal, D.L., Burress, C.N., Shumway, W. et al. 2009. Combining Proven Anti-Sag Technologies for HP/HT North Sea Applications: Clay-Free Oil-Based Fluid and Synthetic, Sub-Micron Weight Material. Paper SPE 119378-MS presented at the SPE/IADC Drilling Conference and Exhibition, Amsterdam, The Netherlands, 17–19 March

De Stefano, G., Stamatakis, E., and Young, S. 2013. Development and Application of Ultra-HTHP Drilling Fluids, paper SPE/OMC 2013-104 presented at Offshore Mediterranean Conference and Exhibition, Ravenna, Italy, 20-22 March.

Elkatany, S.M., Nasr-El-Din, H., and Al Moajil, A. 2012. Evaluation of a New Environmentally Friendly Treatment to Remove Mn3O4 Filter Cake, paper IADC/SPE 156451 presented at the Asia Pacific Drilling Technology Conference and Exhibition, Tianjin, China, 9-11 July.

Elkatatny, S. M, Mahmoud, M.A., and Nasr-El-Din, H.A. 2012. Characterization of Filter Cake Generated by Water-Based Drilling Fluids Using Ct Scan. SPE Drilling & Completion 27 (2): 282-293. SPE-144098-PA.

Elkatatny, S.M., Xiao, J., Nasr-El-Din, H.A. et al. 2013. Using Hydrochloric Acid to Remove Ilmenite Water-Based Filter Cake in HP/HT Applications, paper SPE 165181 presented at the SPE European Formation Damage Conference & Exhibition, Noordwijk, The Netherlands, 5-7 June.

Elkatatny, S.M., Nasr-El-Din, H.A., and Al-Bagoury, M. 2012. Evaluation of Ilmenite as Weighting Material in Water-Based Drilling Fluids for HP/HT Applications, paper SPE presented at the SPE Kuwait International Petroleum Conference and Exhibition, Kuwait City, Kuwait, 10-12 December.

El-Monier, E. A. and Nasr-El-Din, H. A. 2010. A New Environmentally Friendly Clay Stabilizer. SPE Prod & Oper. 28 (2): 145-153. SPE-136061-PA.

Golis, S.W. 1984. Oil Mud Techniques Improve Performance in Deep, Hostile Environment Wells, paper SPE 13156 presented at the SPE Annual Technical Conference and Exhibition, Houston, Texas, USA 16-19 September.

Guo, H., Vocken, J., Opstal, T., et al. 2012. Investigation of the Mitigation of Lost Circulation in Oil-Based Drilling Fluids Using Additives. Paper SPE 151751 presented at the International Symposium and Exhibition on Formation Damage Control, Lafayette, Louisiana, USA, 15-17 February.

Gusler, W., Pless, M., Maxey, J., Grover, and P., Perez, J.: "A New Extreme-HP/HT Viscometer for New Drilling Fluid Challenges," paper SPE 99009 presented at the 2006 IADC/SPE Drilling Conference, Miami, Florida, USA 21-23 February.

Ibeh, C. S. 2007. Investigation on the Effects of Ultra-High Pressure and Temperature on the Rheological Properties of Oil-based Drilling Fluids. Master of Science Thesis, Texas A&M University.

Kageson-Lee, N., Watson, R., and Prebensen, O.I. 2007. Formation Damage Observations on Oil-Based-Fluid System Weighted with Treated Micronized Barite, paper SPE 107802 presented at the European Formation Damage Conference, Scheveningen, The Netherlands, 30 May – 1 June.

Khatib, Z., 1994. Prediction of Formation Damage Due to Suspended Solids; Modeling Approach of Filter Cake Buildup in Injectors, paper SPE 28488 presented at the Annual Technical Conference and Exhibition, New Orleans, Louisiana, USA, 25-28 September.

Kulkarni, D., Maghrabi, S., and Wagle, V. 2014. Synergistic Chemistry Tailors Invert Emulsion Fluids (IEF) with Consistent Rheology to Minimize Equivalent Circulating Density (ECD) Fluctuations, paper SPE 171695 presented at the Abu Dhabi International Petroleum Exhibition and Conference, Abu Dhabi, UAE, 10-13 November.

Mahrous, R., Barkmann, T., Elshout, N. et al. 2016. Innovative Low-ECD Organo-Clay-Free Invert Emulsion Fluid OCF-IEF System Helped Operations Hit Target, paper SPE-180633 presented at the IADC/SPE Asia Pacific Drilling Technology Conference Singapore, 22-24 August.

Martini, L., Ripa, G., Pellicanò, et al. 2017. Clay-Free Drill-In Fluid Reduces the Total Cost of Ownership While Exceeding Production Expectations, paper OMC-2017-648 presented at the Offshore Mediterranean Conference, Ravenna, Italy, 29-31 March.

Mas, M., Tapin, T., Marquez, R. et al. 1999. A New High-Temperature Oil-Based Drilling Fluid, paper SPE 53941 presented at the Latin American and Caribbean Petroleum Engineering Conference, Caracas, Venezuela, 21-23 April.

Mao, H., Qiu Z., and Xie, B. 2016. Development and Application of Utra-High Temperature Drilling Fluids in Offshore Oilfield Around Bohai Sea Bay, China, paper SPE/OTC 26384 presented at the Offshore Technology Conference Asia, Kuala Lumpur, Malaysia, 22-25 March.

McKinney, L.K., Iyoho, W., and Azar, J.J. 1988. Formation Damage Due to Synthetic Oil Mud Filtrates at Elevated Temperatures and Pressures, paper SPE 17162 presented at SPE Formation Damage Control Symposium, Bakersfield, California, USA 8-9 February.

Melbouci, M. and Sau Arjun, C. 2006. Water-Based Drilling Fluids. U.S. patent No. 20060019834 (January 2006).

Methven, N., and Baumann, R. 1972. Performance of Oil Muds at High Temperatures, paper SPE 3743 presented at SPE European Spring Meeting, Amsterdam, Netherlands, 16-18 May.

Mitchell, R. F., S. Z. Miska. 2011. Fundamentals of Drilling Engineering, Vol. 12: SPE Textbook Series, Society of Petroleum Engineers (Reprint).

Mohammed, A.H. 2001. Effect of Drilling Fluid Particle Sizes on Formation Damage: Application to Horizontal Well, M.S thesis, King Fahad University of Petroleum & Minerals, Dhuhran, Saudi Arabia.

Morton, E.K., Bomar, B.B., Schiller, M.W. et al. 2005. Selection and Evaluation Criteria for High-Performance Drilling Fluids, paper SPE 96342 presented at SPE Annual Technical Conference and Exhibition, Dallas, Texas, USA, 9-12 October.

Njobuenwu, D.O. and Wobo, C.A. Effect of Drilled Solids on Drilling Rate and Performance. Journal of Petroleum Science and Engineering, 55, 3-4: 271-276 (February 2007).

Novelline, R.A. 2004. Squire's Fundamentals of Radiology. 6th. Harvard University Press.

Payne, M. L., and Abbassian, F. 1997. Advanced Torque and Drag Considerations in Extended-Reach Wells. Society of Petroleum Engineers, paper SPE 35102 presented at the IADC/SPE Drilling Conference, New Orleans, Louisiana, USA, 15-18 March.

Rabia, H. 2001. Chapter 7- Drilling Fluids. In Well Engineering & Construction, 197-230.

Rheological Models. Schlumberger, http://www.glossary.oilfield.slb.com/. Downloaded 23 April 2018.

Rødsjø, M., and Akutsu, E. 2013. Case History: Clay-Free Invert Fluid in Norwegian High-Temperature Well Provides Consistent Low ECD Profile, paper SPE 166538 presented at the SPE Offshore Europe Oil and Gas Conference and Exhibition, Aberdeen, UK, 3-6 September.

Rostami, A., and Nasr-El-Din, H. 2010. A New Technology for Filter Cake Removal, paper SPE 136400 presented at the SPE Russian Oil and Gas Technical Conference and Exhibition, Moscow, Russia, 26-28 October.

Schmidt, D., Roos, A., and Cline, J. 1987. Interaction of Water with Organophilic Clay in Base Oils to Build Viscosity, paper SPE 16683 presented at the SPE Annual Technical Conference and Exhibition, Dallas, Texas, 27-30 September.

Shah, S. N., N. H. Shanker, and C. C. Ogugbue. 2010. Future Challenges of Drilling Fluids and Their Rheological Measurements, paper AADE-10-DF-HO-41 presented at the AADE Fluids Conference and Exhibition, Houston, Texas, USA, 13-15 June.

Soliman, A.A., 1995. Oil Base Mud in High Pressure, High Temperature Well, paper SPE 29864 presented at the Middle East Oil Show, Bahrain, 11-14 March.

Tovar, J., Azar, J.J., and Sarma, D.S. 1994. Formation Damage Studies on Reservoir Rocks Using Water-Base and Oil-Base Muds, paper SPE 27349 presented at the International Symposium on Formation Damage Control, Lafayette, Louisiana, USA, 7-10 February.

Ventresca, M.L., Betancourt, J., Castillo, J., et al. 1995. Chemical System for Treating Formation Damage Induced by Inverted Oil Muds, paper SPE 30125 presented at the European Formation Damage Conference, The Hague, Netherlands, 15-16 May.

Wagle, V., Maghrabi, S., and Kulkarni, D., 2013. Formulating Sag-Resistant, Low-Gravity Solids-Free Invert Emulsion Fluids, paper SPE 164200 presented at the Middle East Oil and Gas Show and Conference, Manama, Bahrain, 10-13 March.

Wellington, S.L. and Vinegar, H.J. 1987. X-Ray Computerized Tomography. Journal of Petroleum Technology 39 (8): 885-898. SPE-16983-PA.

Xiao, J., Nasr-El-Din, H., and Al-Bagoury, M. 2013. Evaluation of micronized Ilmenite as a Weighting Material in Oil-Based Drilling Fluids for HP/HT Applications, paper SPE 165184 presented at the European Formation Damage Conference and Exhibition, Noordwyk, The Netherlands, 5-7 June.

Xiao, J., Nasr-El-Din, H., and Al-Bagoury, M. 2015. Removal of Ilmenite Oil-based Filter Cake under HP/HT Conditions Using Hydrochloric Acid, paper SPE 175728 presented at the North Africa Technical Conference and Exhibition, Cairo, Egypt, 14-16 September.

Xie, J. 2001. Models for Filtration During Drilling, Completion and Stimulation Operations. PhD dissertation, The University of Texas, Austin, Texas.

Xie, S., Deng, H., Wang, R. et al. 2013. Useful Recycling and Safe Disposal Technology of Waste Oil Drilling Fluids and Its Application, paper SPE/IPTC 16623 presented at the International Petroleum Technology Conference, Beijing, China, 26-28 March.